Catalysis Science & Technology

Accepted Manuscript

ROYAL SOCIETY OF CHEMISTRY

www.rsc.org/catalysis

The nickel supplies the hydrogen via aqueous phase reforming to the catalytic hydrogenolysis of glycerol.

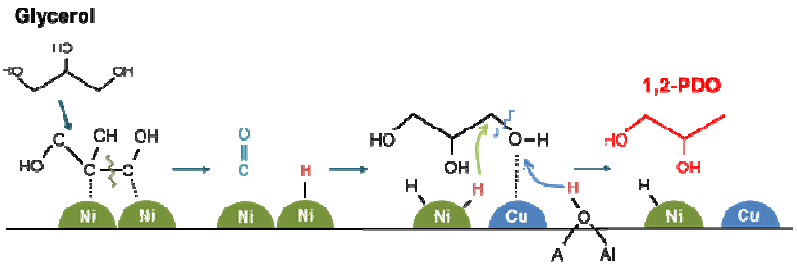

Catalysis Science & Technology

RSCPublishing

ARTICLE

Effect of nickel on catalytic behaviour of bimetallic Cu-Ni catalyst supported on mesoporous alumina for the hydrogenolysis of glycerol to 1,2-propanediol

Cite this: DOI: 10.1039/x0xx00000x

Received 00th January 2014,
Accepted 00th January 2014

DOI: 10.1039/x0xx00000x

www.rsc.org/

Yang Sik Yun[†], Dae Sung Park[†], and Jongheop Yi*

The catalytic conversion of glycerol to 1,2-propanediol by hydrogenolysis has a potential use in the commercial biomass industry. However, the high hydrogen pressure required for the reaction is a major drawback. To overcome this limitation, in this study, we added nickel metal to copper-based catalyst for both supplying hydrogen via aqueous-phase reforming (APR) of glycerol and improving selectivity to 1,2-propanediol in hydrogenolysis. The bimetallic Cu-Ni catalyst supported on a mesoporous alumina (MA) was prepared by sol-gel method. The prepared Cu-Ni catalyst contains ordered-mesopores with a high surface area and well-dispersed active sites, as confirmed by BET, TEM, XRD, and TPR. The 9Cu-1Ni/MA (molar ratio of copper to nickel: 9:1) showed the highest catalytic performance among the various xCu-yNi/MA catalysts in a low pressure of H_2. The XPS results showed that the surface ratio of Ni to (Cu+Ni) and $Cu^0/(Cu^0+Cu^{2+})$ is closely related to catalytic performance, selectivity and yield. The effect of nickel on the hydrogen production was experimentally proven by the time-on-stream tests over monometallic (Cu) and bimetallic (Cu-Ni) catalysts in the absence of hydrogen. In case of the absence of H_2, the optimum value of the ratio of Ni to Cu is varied with the conditions in the presence of H_2. The reaction mechanism was proposed over the Cu-Ni bimetallic catalysts for hydrogenolysis with APR of glycerol.

1. Introduction

As a renewable and sustainable energy source, biodiesel has been an attractive biomass material replacing petroleum-derived diesel fuel. Biodiesel is produced by the transesterification of vegetable oil-based fatty acids, with a major byproduct, glycerol (10 wt.% of production). In recent years, large amounts of low-cost glycerol have been produced as a byproduct with the expanding demand for biodiesel.[1] Thus, the utilization of glycerol for the production of value-added chemicals has become a significant issue. A number of catalytic processes for conversion of glycerol to value-added chemicals has been reported in recently published papers.[2-4] Among the several methods for transformations of glycerol, the hydrogenolysis to 1,2-propanediol (1,2-PDO) has been of interest as a route to the chemical conversion of glycerol due to its reduction process of high O/C content. 1,2-PDO can be used as a component of biodegradable functional fluids such as de-icing reagents, antifreeze and coolants, and as precursors in the synthesis of unsaturated polyester molecules and pharmaceuticals.[5] Therefore, the catalytic hydrogenolysis of glycerol to 1,2-PDO has a great potential for cost-effective process.

Cu metal catalysts have shown superior performance in terms of the selectivity of the hydrogenolysis reaction. It has intrinsic ability to catalyze the cleavage of C-O bonds in presence of H_2 and its relatively poor activity in catalyzing the cleavage of C-C bonds.[6-8] In attempts to enhance the activity, selectivity, and hydrogen utilization of metallic Cu, various Cu-based bimetallic catalysts, such as Cu-Cr, Cu-Zn, Cu-Al, Cu-Mg, and Cu-Ag, have been studied[7,9-12]. In particular, copper chromite shows a very good performance in the hydrogenolysis of glycerol to 1,2-PDO and has a potential for a use in a commercial process in the industry. However, the major drawbacks including the need for a high hydrogen pressure to obtain high yields of 1,2-PDO and the low selectivity of Cu-X bimetallic catalysts must be overcome for commercial use. Furthermore, A high hydrogen pressure inevitably leads to an increase in operating costs. Recently, in attempts to decrease hydrogen pressure, several researchers have examined the possible use of the aqueous phase reforming of glycerol which can serve as an in-situ source of hydrogen in the hydrogenolysis of glycerol to 1,2-PDO. A noble

metal catalyst supported on an acidic support, such as Pt/NaY, Pt/Al_2O_3, and Ru/Al_2O_3 were examined in the past and showed a relatively good performance for conversion and selectivity.[13,14] As an alternate strategy to supply *in-situ* generated hydrogen, hydrogen donor molecules were added to the reactant with a hydrogenation catalyst in a batch or in a continuous reactor.[15] Using these approaches, the developed catalyst and the system showed good catalytic activity. However, other problems were introduced, namely that when a noble metal is used in the catalytic system, an additional separation process is necessary. Therefore, the hydrogenolysis of glycerol at a lower hydrogen pressure without a noble metal or additive hydrogen donor would be highly desirable in terms of developing a commercially acceptable catalytic system.

Herein, to systematically explore the concept of the *in-situ* production of hydrogen and the hydrogenolysis reaction, we developed a Cu-Ni bimetallic catalyst supported on mesoporous alumina (Cu-Ni/MA). By a one-step sol-gel method with a controlled hydrolysis rate, active metals were highly dispersed on mesoporous alumina. Nano-sized metallic Cu particles selectively cleaved C-O bonds, facilitating the hydrogenolysis of glycerol. Ni metal supported on the alumina was chosen to promote the aqueous phase reforming of glycerol to generate hydrogen and enhance the utilization of hydrogen. Moreover, we investigated the reducibility of metallic Cu and the surface composition of the catalyst varying the Cu:Ni ratios. The findings indicated that the surface ratios of $Cu^0/(Cu^0+Cu^{2+})$, which represents reducibility, and Ni/(Ni+Cu) were the crucial factors in determining the catalytic performance. Furthermore, a mechanistic study revealed that the aqueous phase reforming of glycerol occurred on the Ni sites in the bimetallic catalysts, leading to an enhanced catalytic performance by supplying additional hydrogen.

2. Experimental

2.1. Preparation of Cu-Ni catalysts supported on mesoporous alumina (Cu-Ni/MA)

The Cu-Ni/MA catalysts were synthesized by an one-step sol-gel method[16,17] using aluminum sec-butoxide($Al(sec\text{-}BuO)_3$, Sigma Aldrich) as an aluminum source with controlling the hydrolysis rate via a post-hydrolysis method. Lauric acid was used as a surfactant, and copper nitrate ($Cu(NO_3)_2{\cdot}2.5H_2O$, Sigma Aldrich) and nickel nitrate ($Ni(NO_3)_2{\cdot}6H_2O$, Sigma Aldrich) were mixed with the surfactant in an organic solution. First two solutions, the aluminum source and metal precursors with the surfactant dissolved in sec-butyl alcohol (Fluka) respectively, were prepared. The two solutions were then mixed with vigorous stirring. A series of Cu-Ni/MA bimetallic catalysts were prepared by controlling the molar ratio of copper and nickel at 10:0, 9:1, 7:3, 5:5, and 0:10, and the total loading amount of xCu-yNi was 33 wt% in the xCu-yNi/MA catalysts. After 30 min, micelles were formed by the interaction between the surfactant and the metal precursors. A small amount of water was slowly added dropwise to the solutions at a rate of 0.2 ml min^{-1} for post-hydrolysis until a blue and green precipitate was formed. The samples were stirred for a further 12 h, and then it was dried at 353 K for 24 h. The solid product was finally calcined for 4 h at 823 K in air. Various ratio-controlled xCu-yNi/MA catalysts were denominated to 10Cu/MA, 9Cu-1Ni/MA, 7Cu-3Ni/MA, 5Cu-5-Ni/MA, and 10Ni/MA.

2.2. Catalyst characterization

The catalysts were characterized by various methods, as described below. Adsorption isotherms of nitrogen were obtained with an ASAP2010 (Micromeritics) instrument. Pore size distribution was determined by the BJH method applied to the desorption branch of the nitrogen isotherm. The surface morphology and particle size of the catalyst were examined by high-resolution transmission electron microscopy (HR-TEM: 300 kV, JEOL, JEM-3010). X-ray diffraction (XRD) data for the catalysts were collected by means of an X-ray diffractometer (XRD, D-Max2500-PC, Rigaku Corp.) using Cu Kα (λ=1.5405 Å) radiation at 50 kV and 100 mA. To examine the reducibility of the catalysts, TPR (temperature-programmed reduction, AutoChem II, Micrometritics) was performed using 10% hydrogen in argon with 1 gram of catalyst in a conventional TPR set-up. The temperature was linearly ramped up to 1073 K at a rate of 10 K min^{-1}. The utilization of hydrogen by the catalysts was tested by H_2-TPD (temperature-programmed desorption, AutoChem II, Micrometritics) with a TCD (thermal conductivity detector). The catalysts were reduced at 773 K for 3 h with 10% H_2/N_2 gas. Under these conditions, the catalysts were partially saturated with hydrogen. The temperature of the reduced catalyst was decreased to ambient temperature and a stream of N_2 (30 ml min^{-1}) was then used to physically remove the adsorbed H_2. The measurements were conducted in flowing N_2 from ambient temperature to 1073 K at a ramping rate of 10 K min^{-1}. The acid properties of the catalysts were measured by NH_3-TPD (temperature-programmed desorption, AutoChem II, Micrometritics) with a thermal conductivity detector (TCD). NH_3 adsorption step was carried out at ambient temperature. The NH_3 that was physically adsorbed on the catalyst was removed by hearing at 373 K for 1 h in the presence of an inert gas (He). The signals were measured in He flow from room temperature to 1073 K at a ramping rate of 10 K min^{-1}. The copper metal area were determined by the dissociative N_2O decomposition method using an AutoChem 2920 (Micromeritics, USA). In an each experiment, the catalyst was placed in a U-shaped quartz reactor and in situ reduced in a flow of H_2/Ar at 773 K for 3h. And then, the catalyst was exposed to N_2O gas at 333 K for 1h, resulting in oxidation from Cu to Cu_2O. Finally, s-TPR was performed on the freshly oxidized Cu_2O surface to reduce the Cu_2O to Cu, increasing the temperature up to 723 K with a rate of 10 K min^{-1}. Copper surface area was calculated referring to the previous reported paper.[18] After the hydrogenolysis of glycerol, the amount of copper or nickel that was leached from the system was analyzed by inductively coupled plasma-Mass (ICP-Mass) Spectrometer (PERKIN-ELMER SCIEX, ELAN 6100).

2.3. Catalytic activity for the hydrogenolysis of glycerol

The reactions of the catalysts with glycerol were carried out in a Teflon-lined stainless steel autoclave reactor (100 mL). In each reaction, 50 g of an aqueous glycerol solution (80 wt.% glycerol solution) and 0.02 mol of active metal (Cu, Ni) in the catalysts were loaded in the reactor. Prior to the reaction, the catalysts were reduced in a stream of 10% H_2/N_2 at 773 K for 3 h. The reactor was then flushed 3 times with N_2 to remove the ambient air. The hydrogenolysis of glycerol was performed with the reduced catalysts at a temperature of 493 K for 10 h with vigorous stirring (500 rpm). The reactant and product in the liquid phase were analyzed using an off-line gas chromatograph (GC, YL 6200, Younglin Instrument) equipped with a flame ionization detector (FID) and a capillary column (HP-INNOWAX, 30 m × 320 mm × 0.5 μm). The gaseous

products from the batch reactor were passed through a condenser at 278 K resulting in separation of gas and liquid phases after the reaction. The gas-phase products were analysed by a gas chromatograph (GC, YL 6100, Younglin Instrument) equipped with TCD detector and packed column (ShinCarbon ST). The acquired experimental data were analyzed using the following equations:

Glycerol conversion:

- Glycerol conversion:

$$\text{conversion}\ (\%) = \frac{\text{moles of glycerol reacted}}{\text{initial moles of glycerol}} \times 100$$

- Glycerol conversion into gas:

$$X_G(\%) = \frac{\text{C atoms in gas products}}{\text{C atomes in feed}} \times 100$$

Selectivity of the liquid and gas-phase products:

- Yield of liquid products:

$$Y_i\ (\%) = \frac{N^{out}{}_{\text{liquid products}}}{N^{in}{}_{\text{Glycerol}}} \times 100$$

- Selectivity to CO_2, CO, and CH_4

$$S_i(\%) = \frac{\text{C atoms in species i}}{\text{C atomes in gas products}} \times 100$$

- Selectivity to hydrogen:

$$S_{H_2}(\%) = \frac{\text{moles of } H_2 \text{ produced}}{\text{C atomes in gas products}} \times \frac{3}{7} \times 100$$

3. Results and discussion

3.1. Characterization of the prepared xCu-yNi/MA catalysts

The pore structure of the reduced xCu-yNi/MA catalysts were characterized by N_2 adsorption-desorption isotherms as shown in Fig. 1 and the corresponding textural properties are summarized in Table 1. All of the tested Cu-Ni samples exhibited a type IV isotherm with a hysteresis loop in the relative pressure range of 0.4-0.8, implying the presence of a meso-structure. The samples had a uniform pore size within a range of 3-6 nm, as confirmed by pore size distribution curves in Fig. 1B. The prepared catalysts showed high BET surface areas of over ca. 160 $m^2\ g^{-1}$ due to their unique structure. However, as the ratio of Cu to Ni increases, the isotherms of the catalysts exhibit a slightly different hysteresis loop with a decrease in both surface area and pore volume. This result represents that metallic Cu area is varied in xCu-yNi/MA catalysts. As seen in Table 2, the Cu metal area was also increased as increasing the amount of Ni. Concerning on pore size distribution, monometallic (10Cu/MA and 10Ni/MA) catalysts showed symmetric pore size distribution curve as shown in Fig. 1B. However, relatively broad and asymmetric curves were observed after the addition of Ni. It is due to the different interaction between metal ions (Cu and Ni) with micelle complex in sol-gel process.[19] The pore size of the prepared catalysts decreased with the increase in Cu contents because of the poor interaction of surfactant molecules with Cu ions and partial pore blocking by metallic Cu, as evidenced by the TGA and DTA curves.

Fig. 2 shows the TG and DTA curves for the as-synthesized 10Cu/

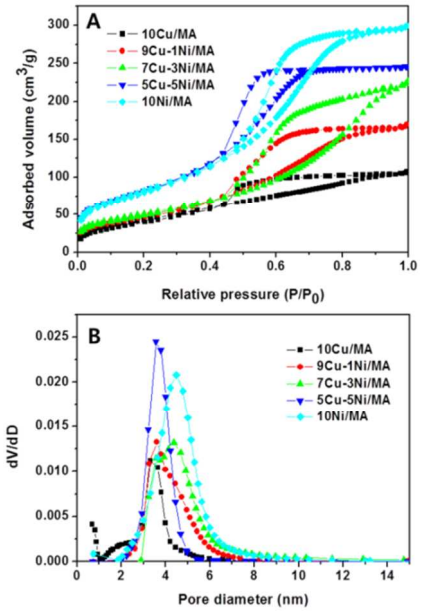

Fig. 1 (A) Isotherm curve and (B) pore size distribution of the various xCu-yNi/MA catalysts by N_2 adsorption-desorption experiment.

Table 1 BET surface area and pore volume of the various xCu-yNi/MA catalysts by N_2 adsorption-desorption experiment.

Catalyst	BET surface area (m^2/g)	Pore size (nm)	Pore Volume (cm^3/g)
10Cu/MA	161.6	3.3	0.17
9Cu-1Ni/MA	179.1	3.5	0.26
7Cu-3Ni/MA	186	4.3	0.35
5Cu-5Ni/MA	219	3.6	0.38
10Ni/MA	306.9	4.6	0.47

MA and 10Ni/MA catalysts. These data was collected in order to get insights on the nature of the interactions between metal ions and surfactant. The weight loss at temperatures of up to 500 K can be attributed to the removal of the residual organic solvent and adsorbed water molecules. The point where the slope becomes steep, at around 500 K, can be attributed to the loss of surfactant molecules. A similar trend was observed in the weight loss curves of both catalysts for temperatures up to 500 K. However, the percentage of weight loss of the as-synthesized 10Ni/MA catalyst was higher than that for the as-synthesized 10Cu/MA catalyst. This result can be attributed to the good interactions of surfactant molecules with Ni ions, compared to Cu ions, leading to the formation of well-developed micelle complexes.[17] The DTA curve for the as-synthesized 10Ni/MA catalyst, which showed a large exothermic peak at around 580 K, caused by the removal of surfactant, provides further evidence for this good interaction between surfactant molecules and Ni ions.

Fig. 3 shows TEM images of the reduced xCu-yNi/MA and 9Cu-1Ni/ Al_2O_3 catalysts. All of the catalysts that were prepared by the sol-gel method exhibited a wormhole-like structure with meso-size pores, consistent with the N_2 adsorption-desorption data. Highly dispersed metal particles with a size of 20-30 nm were observed in the case of the 9Cu-1Ni/MA catalyst which contains a large portion of Cu. On the other hand, aggregated metal particles were found in 9Cu-1Ni/Al_2O_3 catalyst which was prepared by the impregnation method. The Cu metal area and dispersion of 9Cu-1Ni/Al_2O_3 (212.6

m^2g^{-1}, 31.6 %) were lower than that of 9Cu-1Ni/MA catalyst (292.6 m^2g^{-1}, 43.4 %). This indicates that our preparation method is effecti-

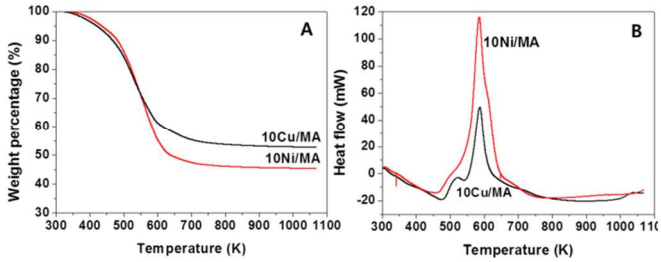

Fig. 2 (A) TGA patterns and (B) heat flow curves of the 10Cu/MA and 10Ni/MA catalysts before calcination process.

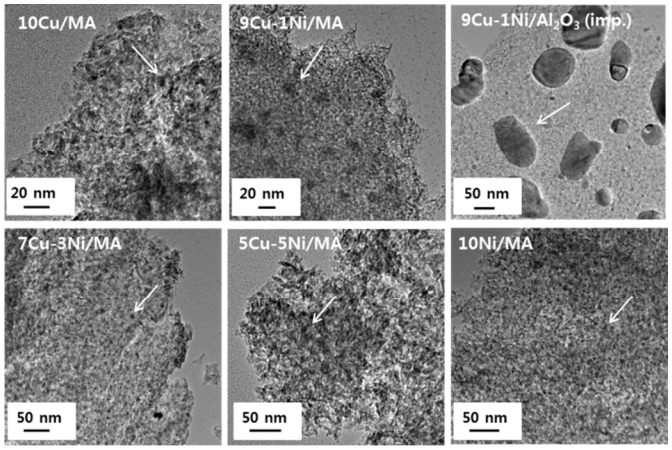

Fig. 3 TEM images of the xCu-yNi/MA catalysts, and 9Cu-1Ni/Al_2O_3 catalyst prepared by impregnation method. Arrows indicate metal particles.

ve in terms of dispersing active metal particles. Meanwhile, smaller metallic particles were confirmed to be present in other catalysts that contain a lower content of Cu than that of 9Cu-1Ni/MA due to the high dispersity of the active metal species.

The crystalline phases of the xCu-yNi/MA catalysts were investigated by X-ray diffraction measurement. Fig. 4 shows XRD patterns of the calcined (A and B) and reduced (C and D) xCu-yNi/MA catalysts, respectively. The diffraction patterns of the calcined xCu-yNi/MA catalysts exhibit no characteristic peaks for metals corresponding to Cu, Ni, except a set of peaks at 37.2 °, 45.6 °, and 66.9 °, which are characteristic of γ-Al_2O_3 even for catalysts with at high content of Cu and Ni in catalysts.[16] In the region within 2θ =30-50° (Fig. 4B), featureless peaks at 2θ= 35.5 °, 38.73 ° and 48.7 ° corresponding to CuO[20], and 37.0 ° and 43.3 ° corresponding to NiO[15] were observed in the diffraction patterns of the calcined catalysts. This suggests that the method used to prepare these catalysts results in small-sized metal species. The weak signal at 2θ= 38.8 °, corresponds to the presence of crystalline $CuAl_2O_4$[21] in the 10Cu/MA catalyst, indicating that a part of the CuO species where slightly transformed into a $CuAl_2O_4$ phase during the calcination process. Similar to the calcined catalysts, the characteristic peaks for γ-Al_2O_3 were also detected in catalysts that were reduced at 773 K in a H_2 atmosphere. However, in contrast to the calcined catalysts, the XRD patterns of the reduced catalysts exhibited characteristic peaks for metallic Cu (2θ=43.3 ° and 50.4 °)[20] and Ni (2θ=44.5 ° and 51.8 °)[22] indicating that the reduced catalysts have a higher crystallinity compared to those of the calcined catalysts (Fig. 4C and D). Therefore, it was confirmed that through reduction process, the catalysts were in bimetallic phase with highly dispersed Cu and Ni sites, thereby acting as active sites for C-O cleavage (hydrogenolysis) and C-C cleavage (APR of glycerol) respectively.[20,23]

The reduction behavior of the calcined xCu-yNi/MA catalysts was investigated by H_2-TPR and the results are shown in Fig. 5. The inte-

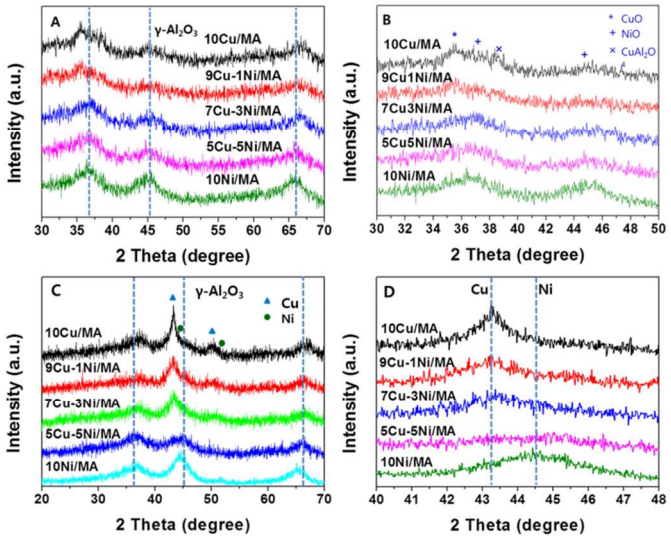

Fig. 4 (A) XRD patterns of the calcined xCu-yNi/MA catalysts, (B) expanded view of the data (A), (C) XRD patterns of reduced catalysts, and (D) expanded view of the data (C).

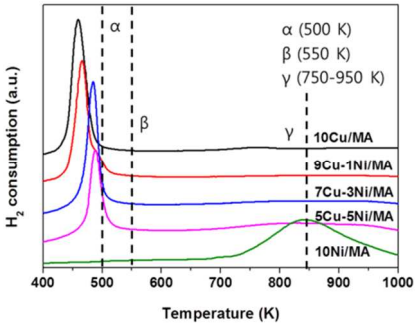

Fig. 5 H_2-TPR profiles of the xCu-yNi/MA catalysts. (Reduced peaks of α: highly dispersed CuO on surface, β: CuO on bulk, and γ: nickel aluminate)

nse peaks in the range of 450-500 K correspond to reduction of CuO species (denoted as α). Broad peaks in the 700-950 K temperature range are due to the reduction of various NiO_x species (denoted as γ). It was reported that the TPR signal attributable to the reduction of CuO species can be shifted, depending on the dispersion of the species on the support.[15] In general, bulk CuO species (denoted as β) start to be reduced at a temperature of around 550 K while highly dispersed CuO species can be reduced at lower temperature (below 500 K) compared to bulk ones.[24,25] Base on this explanation, the CuO species in the prepared catalysts appear to be highly dispersed on the mesoporous alumina, confirming that active sites can be dispersed effectively by this preparation method. The findings also show that the higher the content of Cu species in the bimetallic catalyst, the weaker the interaction between Cu species and support. Hence the CuO can be easily reduced to metallic Cu at high content of Cu species.

The acid properties of the prepared samples were investigated by a NH_3-TPD technique, and the data are shown in Fig. 6. All desorption peaks were observed below 550 K, indicating that the catalysts have the low acid strength appropriate for the conversion of glycerol to acetol rather than to acrolein.[26] According to our observations, the area of the curve corresponding to the amount of acid sites appeared

to change with varying Ni content, but the peak position remained the same. These results can be attributed to variations in the surface area of the catalysts. However, the differences were not sufficient to cause a change of performance due to their low effectiveness. It has been reported that ability of hydrogen utilization of catalyst affects the hydrogenolysis of glycerol.[26] The utilization of hydrogen on the prepared catalysts was examined by H_2-TPD as shown in Fig. 7. No hydrogen desorption peak and a small peak were observed for the 10Ni/MA and 10Cu/MA catalysts. However, the bimetallic catalysts (9Cu-1Ni/MA, 7Cu-3Ni/MA, and 5Cu-5Ni/MA) show a remarkably increased hydrogen desorption peak. This suggests that the hydrogen utilization of the catalyst was enhanced significantly when Ni is added to the 10Cu/MA catalyst. The nickel seems to play the role not only in a higher production of hydrogen, but also in an enhancement of the hydrogen utilization of the catalyst. This enhancement may have a positive influence on the hydrogenolysis of glycerol.

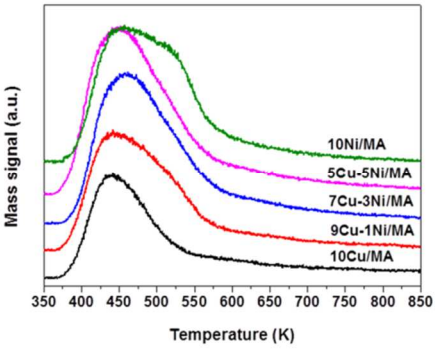

Fig. 6 NH_3-TPD profiles of the xCu-yNi/MA catalysts. (Mass detector, ion current of NH_3 (m/e = 16))

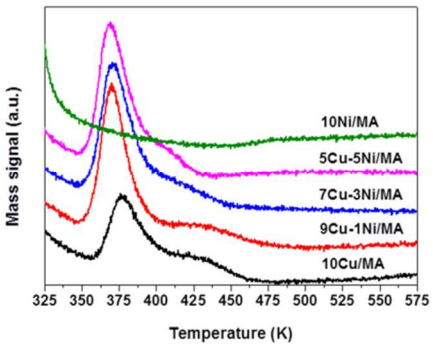

Fig. 7 H_2-TPD profiles of the xCu-yNi /MA catalysts. (Mass detector, ion current of H2 (m/e = 2))

3.2. Catalytic activity of the prepared xCu-yNi/MA catalysts in glycerol hydrogenolysis

A catalytic activity test for the hydrgenolysis of glycerol was carried out using reduced xCu-yNi/MA catalysts with different Cu to Ni ratios. Glycerol conversion, yield and the selectivity to 1,2-PDO are shown in Fig. 8A. 10Cu/MA showed quite high activity (62.4%) and selectivity (52.8%). This result is consistent with previously reported data, showing that metallic Cu is selective for the cleavage of C-O bonds in this reaction.[28] The 10Ni/MA catalyst exhibited the highest conversion of glycerol among the prepared catalysts but had the lowest selectivity for 1,2-PDO due to the fact that it promotes C-C cleavage.[23] A remarkable change in activity and selectivity was observed in bimetallic catalysts. The bimetallic catalysts were less active than monometallic ones, except for 9Cu-1Ni/MA. When Ni added to 10Cu/MA (9Cu-1Ni/MA), the conversion was increased up to 76.6% but selectivity was essentially unchanged compared to 10Cu/MA, resulting in the highest yield (42.4%) of 1,2-PDO. It suggests that H_2 would be produced from the APR of glycerol on metallic Ni and would have a positive effect on the yield of 1,2-PDO. In addition, metallic Ni can facilitate the utilization of active hydrogen in hydrogenation, which would promote the second step, and selectivity were decreased significantly over 7Cu-3Ni/MA and 5Cu-5Ni/MA even lower than monometallic 10Cu/MA. This may be because a decline in the amount of Cu and an increase in that of Ni on the surface layer induced a preferential C-C cleavage rather than C-O cleavage. This result suggests that 9Cu-1Ni/MA has the optimal Cu:Ni ratio for a high activity and selectivity in the hydrogenolysis of glycerol by the ensemble effect. When Ni was added into the Cu monometallic catalyst, the catalytic activity was significantly decreased. This is due to the presence of H_2 and the characteristic of bimetallic catalyst. Gandarias and coworkers also reported that the activity was not increased with increasing in the nickel contents caused by the hydrogen. Under the hydrogen environment, the glycerol was favorably adsorbed on Cu metal, and the adsorption sites on Ni were mostly occupied with the hydrogen.[29,30] Thus, the hydrogenolysis of glycerol is more dominant than aqueous phase reforming in the presence of H_2. Therefore, it has an optimum point of the nickel content on xCu-yNi bimetallic catalyst for the highest conversion of glycerol. It is well known that in bimetallic catalysts, the addition of second metal induces significant changes of both activity and selectivity in catalytic reaction.[22,31-33] For further investigation of the activity on xCu-yNi bimetallic catalysts, the selectivity of the various liquid and gas-phase products was tabulated in Table 2. The selectivity of C<3 products (ethylene

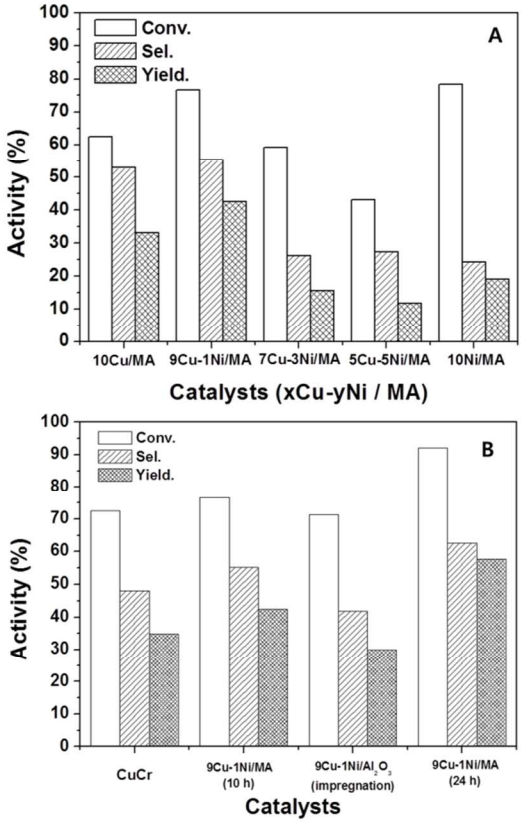

Fig. 8 Catalytic activity test for hydrogenolysis of glycerol in a batch reactor of (A) the xCu-yNi/MA catalysts and (B) $CuCr_2O_4$, 9Cu-1Ni/Al_2O_3 catalysts prepared by sol-gel method and impregnation. (Conditions: 493 K, 40 bar of H_2, 12 h (24 h), 1 g of catalyst, 80 wt% of glycerol solution)

glycol, ethanol, methane) on the xCu-yNi bimetallic catalysts were slightly increased with increasing of the Ni contents. The amount of produced 1-propanol (1-PO) and 2-propanol (2-PO) was rapidly increased after the addition of Ni to the Cu monometallic catalyst. The 1-PO and 2-PO can be produced by additional dehydration and hydrogenation of 1,2-PDO or 1,3-PDO.[30] Therefore, the high selectivity of 1-PO and 2-PO indicates that our catalytic system follows the dehydration-hydrogenation mechanism rather than the glyceraldehyde-based mechanism. It should be noted that the glyceraldehyde was not detected. The conversion of glycerol to the gas-phase products was also decreased with increasing of Ni content on xCu-yNi/MA catalysts. However, on the 10Ni/MA catalyst, much more glycerol was converted to the gas-phase products than other catalysts because of the conversion of glycerol by aqueous phase reforming. These results indicate that the nickel plays a role on promoting the additional dehydration-hydrogenation of produced propylene glycols on xCu-yNi/MA catalysts in the presence of H_2. The C-C cleavage of glycerol is not well occurred over the xCu-yNi catalysts in a pressurized H_2 environment.

Table 2 Composition of the liquid and gas-phase by-products over xCu-yNi/MA catalysts in hydrogenolysis of glycerol. (Conditions: 493 K, 40 bar of H_2, 12 h, 1 g of catalyst, 80 wt% of glycerol solution)

Products	10Cu	9Cu-1Ni	7Cu-3Ni	5Cu-5Ni	10Ni
Liquid-phase (%)					
Formaldehyde	0.1	0.1	0.1	0.1	0.2
Ethanol	1	2.2	2.1	2.5	4.5
1PO + 2 PO	3.6	16	9.6	6.4	2.4
Acetol	3.8	3	4.9	1.7	2.9
EG	2.4	2.1	2.6	2.1	6.5
1,2-PDO	52.8	55.3	26.3	27.3	24.3
Gas-phase (%)					
$X_{glycerol}$	3	1.6	1.5	1.1	10.3
S_{CO2}	13.7	6.6	5.2	9.2	13.8
S_{CO}	5.1	3.2	3.8	5.9	19.5
S_{CH4}	1.3	1.2	1.2	1.6	35.1

In order to confirm the superior catalytic performance of the xCu-yNi/MA catalyst, catalytic tests were performed using copper chromite (CuCr) and Cu-Ni/Al_2O_3 catalysts prepared by the sol-gel and impregnation methods, respectively. It is well known that copper chromite is one of the most effective catalysts for the hydrogenolysis of glycerol to 1,2-PDO after a reduction process when a 1:2 ratio of Cu:Cr is used.[34] In order to check the difference resulting from the preparation methods, 9Cu-1Ni/Al_2O_3 was prepared with the same weight percent of metal on a commercial gamma alumina support and the same ratio of Cu:Ni as was used for 9Cu-1Ni/MA, followed by a reduction process at 773 K for 3 h. Fig. 8B shows the results of a catalytic activity test for the hydrogenolysis of glycerol over CuCr, 9Cu-1Ni/Al_2O_3 (imp.), and 9Cu-1Ni/MA for 12 h and 24 h in a batch reactor. The CuCr exhibited a 72.5% conversion and a 48.1% selectivity, which are slightly lower than those of 9Cu-1Ni/MA. This confirms that 9Cu-1Ni/MA is a highly appropriate catalyst for the hydrogenolysis of glycerol. In the case of 9Cu-1Ni/Al_2O_3 prepared by the impregnation method, a lower conversion of glycerol with a significant decline in selectivity from 55.3% to 41.9% was observed. This observation can be attributed to the poor dispersion of metallic Cu on the alumina support, as confirmed in TEM images (Fig. 3). This result suggests that our preparation method is effective in terms of dispersing the active metal, thereby resulting in the generation of a high performance catalyst. In addition, a high performance was found for 9Cu-1Ni/MA for 24 h, with a yield approaching nearly 60%.

3.3. Effect of the surface ratio of Cu-Ni bimetallic catalysts on glycerol hydrogenolysis

It is well known that the oxidation state of the active site influences its catalytic performance, especially in metallic catalysts.[35,36] Hence, we performed XPS analyses of the reduced catalysts containing Cu species. By this analysis, it is possible to obtain information on how the oxidation state of Cu and its proportion affects catalytic activity. Finally, information can be obtained relative to the reason why the Cu-Ni/MA catalysts with various Cu:Ni ratios exhibit different catalytic performance. The Fig. 9 shows XPS spectra in the $2p_{3/2}$ region of Cu for samples for various Cu/Ni ratios. The area of the XPS spectrum increases with increasing the fraction of Cu in the catalysts, implying that Cu species are abundant on the surface layers. These Cu $2p_{3/2}$ spectra can be divided into three peaks at 932.7 eV, 933.6 eV, which are assigned to metallic Cu, Cu^{2+} in CuO respectively.[37,38] Deconvoluted Cu $2p_{3/2}$ spectra of the 10Cu/MA, 9Cu-1Ni/MA, 7Cu-3Ni/MA, 5Cu-5Ni/MA samples are shown in Fig. 9 A, B, C, and D, respectively. The spectra of the bimetallic catalysts were deconvoluted mainly by two peaks, metallic Cu and Cu^{2+} from CuO. The relative surface ratios of the Cu^0 to Cu^{2+} in the prepared catalysts measured by XPS are listed in Table 2. A higher $Cu^0/(Cu^0+Cu^{2+})$ ratio was obtained in cases of bimetallic catalysts with higher Cu contents, implying that reducibility increases with increasing the fraction of Cu, consistent with the TPR data. The 10Cu/MA catalyst showed a lower reducibility than that for 9Cu-1Ni/MA. This result means that a small amount of nickel leads to an enhancement in the reducibility of surface copper oxide on mesoporous alumina-supported Cu. On the basis of the calculated data in Table 2, we developed a correlation plot for the surface atomic % of Ni with $Cu^0/(Cu^0+Cu^{2+})$ ratios on the surface layers of bimetallic catalysts versus their catalytic performance. The data points were from the results of XPS analyses and activity tests involving the 10Cu/MA, 9Cu-1Ni/MA, 7Cu-3Ni/MA and 5Cu-5Ni/MA catalysts. The 9Cu-1Ni/MA catalyst had the highest $Cu^0/(Cu^0+Cu^{2+})$ ratio, as shown in Fig. 10A. It is found that the ratio, reducibility of the Cu species in the catalysts, was closely related to the yield of 1,2-PDO. Furthermore, this result indicates that the role of Ni is not only to supply hydrogen by the aqueous phase reforming of glycerol but also to increase the reducibility of Cu metal.

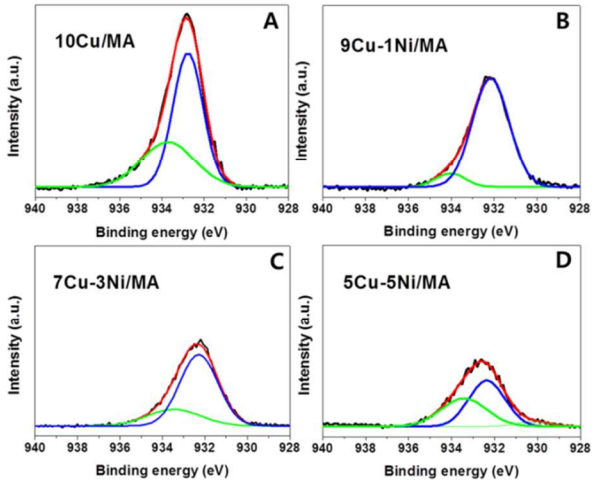

Fig. 9 XPS spectra and their deconvolution spectra of the reduced samples in Cu $2p_{3/2}$ region; (A) 10Cu/MA, (B) 9Cu-1Ni/MA, (C) 7Cu-3Ni/MA, and (D) 5Cu-5Ni/MA.

Table 3 Summary of Cu metal area, Cu/Ni atomic ratio, surface state of Cu from XPS deconvolution data of the xCu-yNi/MA catalysts.

Catalyst	Cu metal area (m^2g^{-1})	Cu/Ni[b]	Ni on surf. (%)[c]	Cu on surf. (%)[c]	Cu^0 (932.7 eV)	Cu^{2+} from CuO (933.6 eV)	Cu^0 / (Cu^0+Cu^{2+})
10Cu/MA	165.2		0	100	2859.2	696.1	0.820
9Cu-1Ni/MA	292.6	9.03	8.07	91.93	2328.5	236.1	0.908
7Cu-3Ni/MA	376.1	2.34	27.38	72.61	1594.3	516.9	0.755
5Cu-5Ni/MA	497.8	1	39.83	60.16	951.5	742.3	0.562

[a] Calculated from H_2-uptake by s-TPR[18], [b]Atomic composition obtained from theoretical calculation. [b]Atomic surface composition obtained from XPS results.

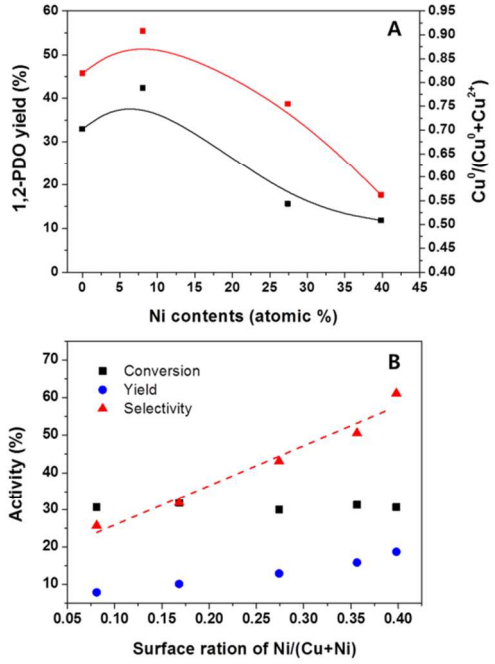

Fig. 10 Correlations of catalytic activity for the glycerol hydrogenolysis (A) with cupper state of surface; $Cu^0/(Cu^0+Cu^{2+})$ and (B) with surface atomic ratio of Ni/(Cu+Ni) of the xCu-yNi/MA catalysts (Surface atomic % of Ni and Cu: 17 and 83 % in 8Cu-2Ni/MA, 33 and 67 % in 6Cu-4Ni/MA by XPS analysis).

Partial pressure of hydrogen is one of important factor to determine catalytic performance.[39] Thus, it can be expected that the *in-situ* supply of hydrogen has a large effect on selectivity for 1,2-PDO. In order to investigate the effect of Ni metal on hydrogen production (which can affect 1,2-PDO selectivity), we developed a correlation plot of the ratio of Ni/Cu+Ni on the surface layers of the samples versus the selectivity. To make the reliability of the correlation plot higher, two additional samples (8Cu-2Ni/MA, 6Cu-4Ni/MA) were prepared and analyzed by XPS and subjected to reaction testing. In addition, the conversion of glycerol for each sample was adjusted to a similar value by controlling reaction time. As shown in Fig. 10B, selectivity for 1,2-PDO increases with an increase in the Ni ratio on the surface layers. This can supports the large influence of hydrogen supply on selectivity for 1,2-PDO in liquid phase glycerol hydrogenolysis. Based on the results from Fig. 10A and B, it appears that reduced Cu contributes to the selective conversion of glycerol to acetol with selective cleavage of C-O bonds and Ni contributes to the increase in selectivity for 1,2-PDO by supplying additional hydrogen. Meanwhile, it is thought that 10Ni/MA, a sole Ni catalyst, is mainly active in the formation of gas phase products rather than the formation of acetol. It can be concluded that the high performance of 9Cu-1Ni/MA may be due to the optimum Cu and Ni ratio on the surface layer for selective C-O bond cleavage and hydrogen production of glycerol APR.

3.4. Durability and reusability of the prepared catalyst

In order to investigate the durability and reusability of the 9Cu-1Ni/MA catalyst, the catalyst was recycled three times after the reaction. For the recycling test, the product obtained using the used catalyst was transferred to a centrifugation tube, and the used catalyst was separated from the liquid-phase product by centrifugation. The used catalyst was then washed with distilled water three times to remove the adsorbed organic species, and then dried at 80 °C for 12 h. In liquid-phase glycerol hydrogenolysis, it was previously reported that the deactivation of active sites is due to the leaching of the metal species, the sintering of active material and the change in the surface state of reduced active metal.[14,40,41] When the reaction is conducted under H_2 pressure, the reaction proceeds via the acetol pathway (fast hydrogenation of the acetol after the rate determining step; glycerol dehydration), and coke deposition does not have a significant effect on the decrease of the active sites.[42] We first checked the leaching of Cu or Ni after the reaction by ICP-MS analysis, which confirmed that the leaching of Cu and Ni ions rarely occurred during the reaction (0.25 ppm of Cu and 0.013 ppm of Ni in aqueous phase products). The results of the recycling test of the 9Cu-1Ni/MA catalyst are shown in Fig. 11. After the first recycle test, the catalyst showed a glycerol conversion of 69.8 % (7 % less than a fresh sample) and a 39.7 % yield of 1,2-PDO (2.7 % less than a fresh sample). As seen in Fig. 12A and B, the particle size of the metallic Cu was slightly larger than a fresh one, and the structure and morphology of the catalyst was not changed after the reaction. However, after the 2nd and 3rd recycling tests, the metallic Cu was rapidly sintered, resulting in the growth of the particle size from 10-20 nm to 40-50 nm. From the XRD patterns, the peak for CuO (Cu^{2+}) was sharply increased and an additional peak of Cu_2O (Cu^+) appeared at 2θ = 42.6 ° (JCPDS 34-1354). This suggests that the reduced metallic copper was oxidized and sintered during the hydrogenolysis of glycerol in the aqueous phase, resulting in the rapid deactivation of the catalyst and a corresponding decrease in activity (57.2% conversion and 33.9 % yield of 1,2-PDO). The morphology of the catalyst was also significantly altered as seen in the image of HR-TEM after the 3rd recycle test. In order to clarify the effect of Ni addition on catalytic stability, recycling tests using monometallic (10Cu/MA) and bimetallic (7Cu-3Ni/MA) catalysts were carried out (Fig. S1). The glycerol conversion of 10Cu/MA

catalyst was higher than that of 7Cu-3Ni/MA. However, the trend was inversed after the 3rd recycling tests. It was also observed that 1,2-PDO selectivity of Cu/MA catalyst decreased while the selectivity of 7Cu-3Ni/MA catalyst for 1,2-PDO main

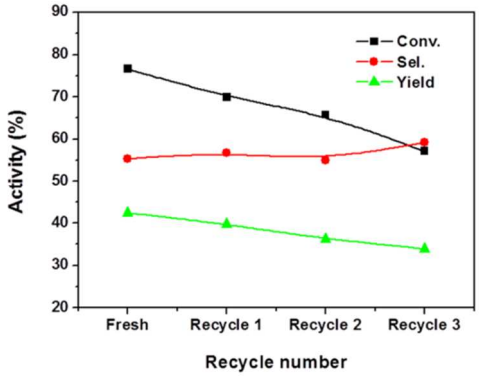

Fig. 11 Catalytic recycling tests of the 9Cu-1Ni/MA catalyst in glycerol hydrogenolysis.

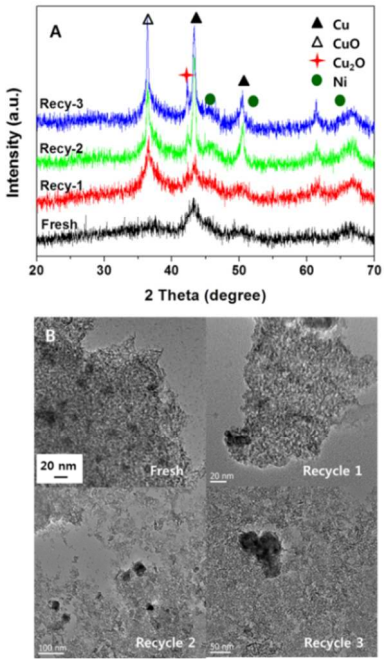

Fig. 12 (A) XRD patterns and (B) HR-TEM images of the 9Cu-1Ni/MA catalyst after recycle tests.

-tained during the recycling test. These results could come from the less deactivation of bimetallic catalyst compared to monometallic catalyst in terms of sintering and oxidation of metallic Cu. These results were confirmed by TEM and XRD analysis (Fig. S2 and S3). It can be concluded that the addition of Ni enhances the catalytic stability in the glycerol hydrogenolysis. Although a severe decrease in the activity was observed, the selectivity of 1,2-PDO was not significantly reduced during the recycle test. This is because the active site that converts glycerol into acetol could be decreased by the sintering process. In addition, the particle size of the metallic nickel was unchanged and its metallic phase was retained during the reaction (as evidenced by XRD data), resulting in maintaining a continuous supply of hydrogen which can affect the selectivity of 1,2-PDO.

3.5. Mechanistic discussion with time-on-stream behavior

To develop a technology that produce 1,2-PDO from glycerol without a need for an external hydrogen source, it is necessary to understand the mechanism responsible for the hydrogenolysis of glycerol to 1,2-PDO. From the previous literature reports, most studies suggested that the conversion of glycerol into 1,2-PDO involves a dehydration to acetol and a subsequent hydrogenation to 1,2-PDO.[43-45] All of the proposed mechanisms are based on the use of a bi-functional catalyst with an additional hydrogen gas for the hydrogenation reaction. Based on this mechanism, Cu in the Cu-Ni/MA selectively cleaves the C-O bonds, leading to the conversion of acetol. In addition, the hydrogen generated from the aqueous phase reforming of glycerol on Ni then is led to the conversion of acetol to 1,2-PDO. Therefore, the acetol to 1,2-PDO step can be controlled by the hydrogen pressure produced from the aqueous phase reaction of glycerol by the Ni metal catalyst. An activity test as time on stream without hydrogen pressure was carried out in order to confirm the proposed mechanistic pathway. Monometallic (10Cu/MA) and bimetallic (7Cu-3Ni/MA) catalysts were used as model catalysts to observe the role of metallic Ni on the hydrogenolysis of glycerol. The conversion of glycerol and product selectivity for 10Cu/MA and 7Cu-3Ni/MA are shown as a function of time in Fig. 13. It was observed that the 1,2-PDO can be produced over only Cu monometallic catalyst in the absence of hydrogen. This is due to the APR of glycerol on the distinct role of Cu and Al in water phase. R. B. Mane et al.[21] revealed that in situ generated hydrogen source from APR of glycerol was dissociatively adsorbed on copper metal, causing hydroxylation of the Al surface. The formaldehyde as an intermediate was detected via dehydrogenation and C-C cleavage of glycerol on Cu. In our case, it seemed that the Cu/MA catalyst also plays a role of C-C cleavage of glycerol via hydroxylation of the mesoporous alumina evidenced by detected formaldehyde although the catalytic efficiency of copper metal is not remarkable. In 7Cu-3Ni/MA, acetol was rapidly produced and then diminished after 3 h with increasing yield of 1,2-PDO, as shown in Fig. 13B. At

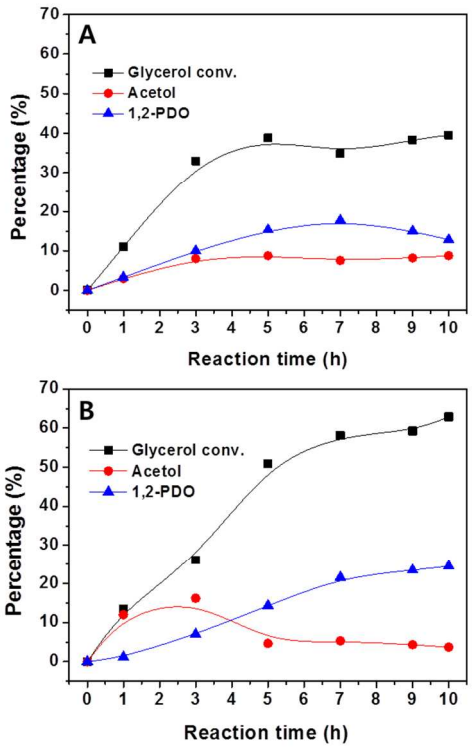

Fig. 13 Time on stream activity for (A) 10Cu/MA and (B) 7Cu-3Ni/MA catalysts without a hydrogen supply in a batch reactor. (Conditions: 220 ^{o}C, no pressure, 1g of catalyst, 80 wt.% of glycerol solution)

the same time, a high conversion was recorded. This indicates that the hydrogenation of acetol involved the use of hydrogen produced by *in-situ* generation on the metallic Ni. However, this reaction pathway does not proceed in the case of a catalyst only containing Cu (Fig. 13A). The conversion of glycerol reached a plateau with a low value after 5 h of reaction time. Selectivity for 1,2,-PDO and acetol was almost maintained. This can be attributed to the fact that there was no hydrogen to be used in the hydrogenation reaction.

The time-on-stream test of the other xCu-yNi/MA catalysts was carried out under the same conditions. As increasing the amount of Ni on xCu-yNi/MA catalysts, the conversion of glycerol was increased due to the aqueous phase reforming (APR) on Ni metal (Figure S4). This result was quite different from the result (Fig. 8) in the presence of H_2. As described before, the relatively low hydrogen pressure enhances the adsorption of glycerol on Ni metal, resulting in increasing the conversion of APR of glycerol. After 10 h, 9Cu-1Ni/MA showed the highest value of selectivity of 1,2-PDO, however, the yield of 1,2-PDO on 7Cu-3Ni/MA was higher than the other catalysts (Table S1). A little amount of the 1-PO and 2-PO was produced. This implies that the additional dehydration-hydrogenation of propylene glycol is not occurred in the absence of hydrogen gas due to the dominant reaction of the aqueous phase reforming on the Ni metal. On the 5Cu-5Ni/MA catalyst, the acetol selectivity and the yield of 1,2-PDO were rapidly decreased, although the hydrogen was produced much more than the other catalysts. By the activity test in the absence of H_2, the ratio of Ni to Cu was an important factor to the high yield of 1,2-PDO. And the optimum value of the ratio of Ni to Cu is different with respect to the pressurized atmosphere; with the presence of hydrogen gas or the absence of hydrogen gas. From these results, it can be confirmed that metallic Cu and Ni catalyses C-O cleavage and glycerol APR to supply hydrogen gas for the reaction.

Previously, Gandarias et al.[15] reported the hydrogenolysis of glycerol over the Cu-Ni bimetallic catalysts using formic acid as a hydrogen donor (CTH, catalytic transfer hydrogen). In their report, 20Ni-15Cu catalyst showed the highest yield of 1,2-PDO among the various xNi-yCu catalysts in a feed of 0.06 $mol_{glycerol}g^{-1}_{cat}$ at 493 K for 16 h. The value of 1,2-PDO yield was larger than that of our prepared catalyst, 7Cu-3Ni/MA, about 10 % (Reaction conditions: 0.43 $mol_{glycerol}g^{-1}_{cat}$, 493 K, 10 h in Fig. 13B). However, the production of 1,2-PDO per gram of catalyst in our system is much larger than that of previously reported system with considering the amount of reacted glycerol. This implies that the aqueous phase reforming (APR) is more effective than CTH to supply the hydrogen to the hydrogenolysis of glycerol. It should be noted that the reaction with CTH needs both the additional hydrogen donor compound and a lot of water with glycerol in the feed. In this case, the efficiency of the unit weight of catalyst is very low. The optimum amount of Ni on Cu-Ni bimetallic catalyst and the reaction pathway are also different in our system because of the high concentration of glycerol. The reaction pathway of glycerol hydrogenolysis is still controversial between dehydrogenation – dehydration – hydrogenation (Montassieret al.[46]) and dehydration – hydrogenation (Dasari et al.[47]) mechanism. In our system, the hydrogenolysis of glycerol is followed by the mechanism of dehydration-hydrogeation route. It is known that the dehydration-hydrogenation route is suitable for the conditions of acidic sites in catalyst, hydrogen pressure and small amount of water in feed.[48] Therefore, at first, the oxygen on terminal OH of glycerol is adsorbed on Cu metal, then the dehydration into the acetol is occurred by the acidic sites of alumina support (Scheme 1). In the absence of Ni, a small amount of 1,2-PDO is produced because of the absence of hydrogen. After the addition of Ni, there are two possible pathways to produce hydrogen by APR of glycerol on Ni metal.[49] Based on the adsorption energy calculation of glycerol,[50,51] both C-C and C-O bonds are formed on the Ni surface. The binding energies and preferred adsorption sites for atomic C and O on various metals are as follows: Pt (C-Metal: -7.42 eV, O-metal: -4.59 eV), Pd (C-Metal: -6.93 eV, O-Metal: -4.49 eV) and Ni (C-Metal: -6.81 eV, O-Metal: -5.60 eV). Therefore, the adsorbed species could be metal-carbons or metal-oxygen bonds. For the formation of metal-carbon (route A), the glycerol first undergoes reversible dehydrogenation steps to be adsorbed on Ni metal.[49] Thus, it is thought that the adsorption of metal-oxygen (route B) is favorably formed in pressurized H_2 environment. Adsorbed hydrogen from APR of glycerol on Ni is delivered to the primary or terminal carbon of the glycerol which is adsorbed onto Cu. After the protonation to terminal OH by the acidic sites, the Cu metal cleavages the C-O bond, then the hydrogen transfer from Ni metal to the terminal carbon at adjacent Cu metal, simultaneously.[42] When the APR is used for the production of hydrogen in glycerol hydrogenoylsis, both ratio control of Cu to Ni and the reaction conditions are significant factors in the production of 1,2-PDO with high yield. In addition, CTH requires an additional donor compound and semi-continuous reactor for high yield of 1,2-PDO.[48] Therefore, the APR is a more effective source of hydrogen for the conversion of glycerol to various polyols.

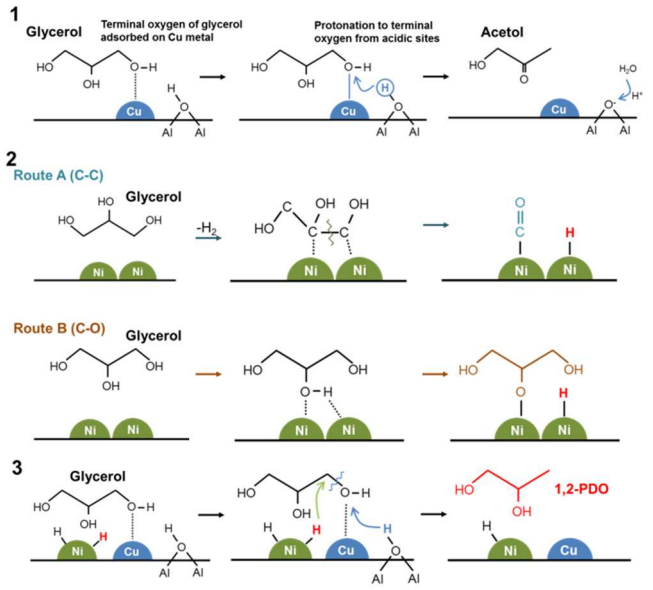

Scheme 1. Proposed reaction pathway for hydrogenolysis of glycerol to 1,2-propanediol with aqueous phase reforming over Cu-Ni/MA catalyst.

4. Conclusions

Cu-Ni bimetallic catalysts supported on mesoporous alumina (MA) with different metal compositions were successfully synthesized using a post-hydrolysis sol-gel method. The Cu-Ni/MA catalysts exhibited mesoporosities and had a relatively high metal dispersion (ca. 33 wt.%), resulting in the formation of nano-sized metal particles. Among the prepared samples, the 9Cu-1Ni/MA catalyst showed the highest catalytic performance, because of the increased hydrogen utilization and the high surface ratio of $Cu^0/(Cu^0+Cu^{2+})$. On the Cu-Ni bimetallic catalysts, the surface ratio of Ni/(Cu+Ni) and the $Cu^0/(Cu^0+Cu^{2+})$ were related to the selectivity and yield in the hydrogenolysis of glycerol to 1,2-PDO. Through the addition of Ni on Cu based catalysts, the reducibility of Cu was increased and hydrogen sources were generated *in-situ* by the aqueous phase reforming of glycerol. The generated hydrogen was subsequently used for the hydrogenation of acetol in the hydrogenolysis of glycerol to 1,2-PDO. By the activity test in the absence of H_2, the ratio of Ni to Cu was an important factor to the high yield of 1,2-PDO. And the optimum value of the ratio of Ni to Cu is different with respect to the pressurized atmosphere; with the presence of hydrogen gas or the absence of hydrogen gas. Their different reaction pathways are proposed over Cu-Ni bimetallic catalysts for the hydrogenolysis of glycerol with aqueous phase reforming.

Acknowledgements

This work was supported by the National Research Foundation of Korea (NRF) grant funded by the Korea government (MEST) (No. 2013R1A2A2A01067164).

Notes and references

World Class University (WCU) Program of Chemical Convergence for Energy & Environment (C2E2), School of Chemical and Biological Engineering, Institute of Chemical Process, College of Engineering, Seoul National University (SNU), Daehak-dong, Gwanak-gu, Seoul 151-741, Republic of Korea

†These authors contributed equally.

**Corresponding author: E-mail: jyi@snu.ac.kr; Tel: +82 2 880 7438*

1 M. G. Musolino, L. A. Scarpino, F. Mauriello and R. Pietropaolo, *ChemSusChem*, 2011, **4**, 1143.
2 B. Katryniok, S. Paul, M. Capron and F. Dumeignil, *ChemSusChem*, 2009, **2**, 719.
3 M. D. Soriano, P. Concepción, J.M.L. Nieto, F. Cavani, S. Guidettib and C. Trevisanut, *Green Chem.*, 2011, **13**, 2954.
4 N. D. Kim, J. R. Park, D. S. Park, B. K. Kwak and J. Yi, *Green Chem.*, 2012, **14**, 2638.
5 Y. Nakagawa and K. Tomishige, *Catal. Sci. Technol.*, 2011, **1**, 179.
6 L. Huang, Y.-L.Zhu, H.-Y.Zheng, Y.-W.Li and Z.-Y.Zeng, *J. Chem. Technol. Biotechnol.*, 2008, **83**, 1670.
7 M. Balaraju, V. Rekha, P.S. Sai Prasad, R.B.N. Prasad and N. Lingaiah, *Catal. Lett.*, 2008, **126**, 119.
8 S. Sato, M. Akiyama, K. Inui and M. Yokota, *Chem. Lett.*, 2009, **38**, 560.
9 Z. Xiao, J. Xiu, X. Wang, B. Zhang, C. T. Williams, D. Su and C. Liang, *Catal Sci. Technol.*, 2013, **3**, 1108.
10 N. D. Kim, S. Oh, J. B. Joo, K. S. Jung and J. Yi, *Korean J. Chem. Eng.*, 2010, **27**, 431.
11 M. Balaraju, K. Jagadeeswaraiah, P. S. S. Prasad and N. Lingaiah, *Catal. Sci. Technol.*, 2012, **2**, 1967.
12 J. Zhou, L Guo, X. Guo, J. Mao and S. Zhang, *Green Chem.*, 2010, **12**, 1835.
13 E. D'Hondt, S. Van de Vyver, B. F. Sels and P. A. Jacobs, *Chem. Commun.*, 2008, 6011.
14 D. Roy, B. Subramaniam and R. V. Chaudhari, *Catal. Today*, 2010, **156**, 31.
15 I. Gandarias, J. Requies, P.L. Arias, U. Armbruster and A. Martin, *J. Catal.*, 2012, **290**, 79.
16 Y. Kim, B. Lee and J. Yi, *Korean J. Chem. Eng.*, 2002, **19**, 908.
17 P. Kim, Y. Kim, H. Kim, I. K. Song and J. Yi, *J. Mol. Catal. A: Chem.*, 2005, **231**, 247.
18 G. V. Sagar, P. V. R. Rao, C. S. Srikanth and K. V. R. Chary, *J. Phys. Chem. B*, 2006, **110**, 13881.
19 P. Kim, Y. Kim, H. Kim, I.K. Song and J. Yi, *Appl. Catal., A*, 2004, **272**, 157.
20 R. B. Mane, S.E. Kondawar, P.S. Niphadkar, P.N. Joshi, K.R. Patil and C. V. Rode, *Catal. Today*, 2012, **198**, 321.
21 R. B. Mane and C. V. Rode, *Green Chem.*, 2012, **14**, 2780.
22 I. Jiménez-Morales, F. Vila, R. Mariscal and A. Jiménez-López, *Appl. Catal., B*, 2012, **117-118**, 254.
23 G. Wen, Y. Xu, H. Ma, Z. Xu and Z. Tian, *Int. J. Hydrogen Energy*, 2008, **33**, 6657.
24 X. Wang, X. Pan, R. Lin, S. Kou, W. Zou and J-X Ma, *Int. J. Hydrogen Energy*, 2012, **35**, 4060.
25 F. E. López-Suárez, A. Bueno-López and M.J. Illán-Gómez, *Appl. Catal., B*, 2008, **84**, 651.
26 A. Alhanash, E.F. Kozhevnikova and I.V. Kozhevnikov, *Appl. Catal., A*, 2010, **378**, 11.
27 B. K. Kwak, D. S. Park, Y. S. Yun and J. Yi, *Catal. Commun.*, 2012, **24**, 90.

28 A. Torres, D. Roy, B. Subramaniam and R.V. Chaudhari, *Ind. Eng. Chem. Res.*, 2010, **49**, 10826.
29 I. Gandarias, S. G. Fernández, M. E. Doukkali, J. Requies and P. L. Arias, *Top. Catal.*, 2013, **56**, 995.
30 I. Gandarias, P. L. Arias, J. Requies, M. B. Güemez and J. L. G. Fierro, *Appl. Catal. B*, 2010, **97**, 248.
31 R. L. Manfro, T. P. M. D. Pires, N. F. Ribeiro and M. M. V. M. Souza, *Catal. Sci. & Technol.*, 2013, **3**, 1278.
32 V. Ponec, *Appl. Catal. A: Gen.*, 2001, **222**, 31.
33 B. Coq and F. Figueras, *Coord. Chem. Rev.*, 1998, **178-180**, 1753.
34 N. D. Kim, S. Oh, J. B. Joo, K. S. Jung and J. Yi, *Top. Catal.*, 2010, **53**, 517.
35 Y. Zhu, W. Lu, H. Li and H. Wan, *J. Catal.*, 2007, **246**, 382.
36 M. S. Kumar, N. Hammer, M. Rønning, A. Holmen, D. Chen, J.C. Walmsley and G. Øye, *J. Catal.*, 2009, **261**, 116.
37 A. Crucq, L. Degols, G. Lienard and A. Frennet, *Stud. Surf. Sci. Catal.*, 1983, **17**, 137.
38 F. Vila, M. Lopez Granados, M. Ojeda, J.L.G. Fierro and R. Mariscal, *Catal. Today*, 2012, **187**, 122.
39 M. A. Dasari, P. Kiatsimkul, W. R. Sutterlin and G. J. Suppes, *Appl. Catal., A*, 2005, **281**, 225.
40 Z. Huang, F. Cui, H. Kang, J. Chen and C. Xia, *Appl. Catal., A*, 2009, **366**, 288.
41 Z. Huang, F. Cui, J. Xue, J. Zuo, J. Chen and C. Xia, *Catal. Today*, 2012, **183**, 42.
42 I. Gandarias, P.L. Arias, J. Requies, M.E. Doukkali and M.B. Güemez, *J. Catal.*, 2011, **282**, 237.
43 J. Chaminand, L. Djakovitch, P. Gallezot, P. Marion, C. Pinel and Cécile Rosier, *Green Chem.*, 2004, **6**, 359.
44 T. Miyazawa, Y. Kusunoki, K. Kunimori and K. Tomishige, *J. Catal.*, 2006, **240**, 213.
45 A. Perosa and P. Tundo, *Ind. Eng. Chem. Res.*, 2005, **44**, 8535.
46 C. Montassier, D. Giraud and J. Barbier, *Heter. Catal.Fine.Chem.*, 1998, 165.
47 C.-W. Chiu, M. A. Dasari and G. J. Suppes, *AIChE J.*, 2006, **52**, 3543.
48 A. Martin, U. Armbruster, I. Gandarias and P. L. Arias, *Eur. J. Lipid Sci. Technol.*, 2013, **115**, 9.
49 R. R. Davda, J. W. Shabaker, G. W. Huber, R. D. Cortright and J. A. Dumesic, *Appl. Catal. B*, 2005, **56**, 171.
50 R. Alcalá, M. Mavrikakis and J. A. Dumesic, *J. Catal.*, 2003, **218**, 178.
51 B. Liu and J. Greeley, *Phys. Chem. Chem. Phys.*, 2013, **15**, 6475.

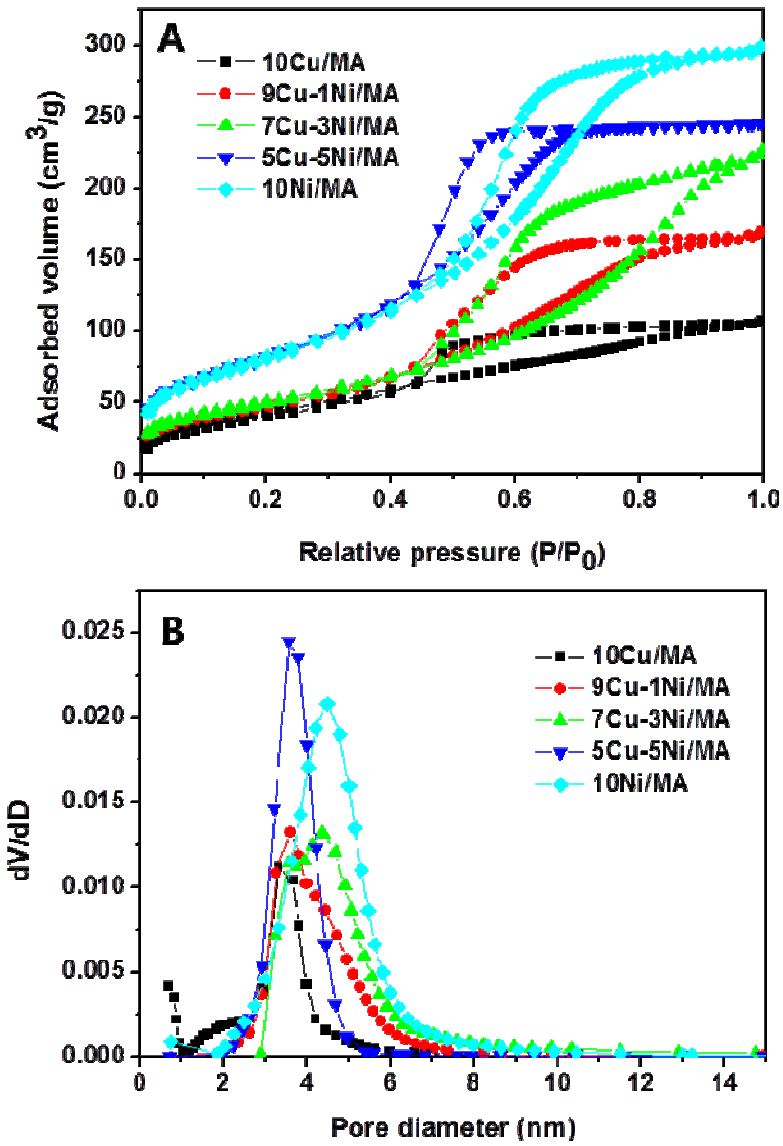

Fig. 1

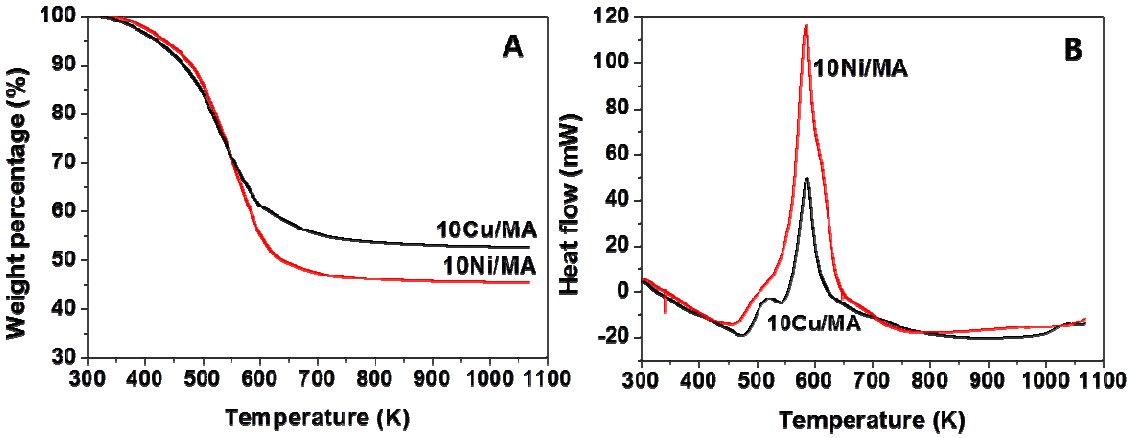

Fig. 2

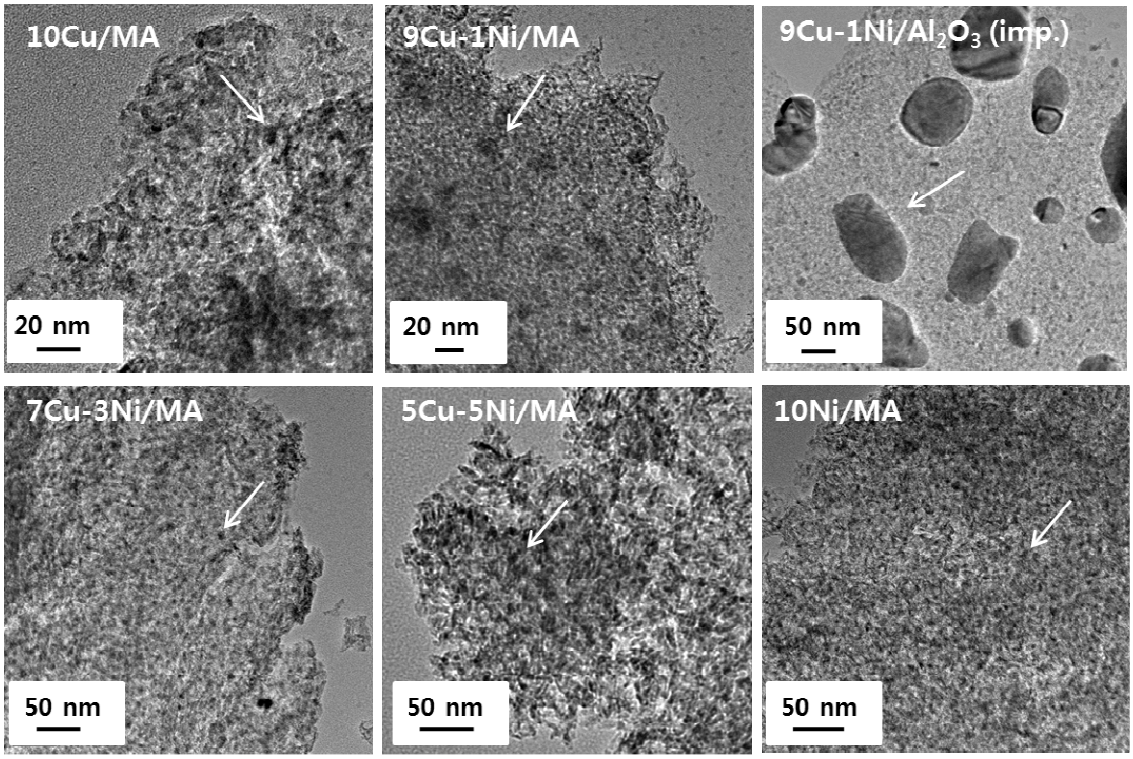

Fig. 3

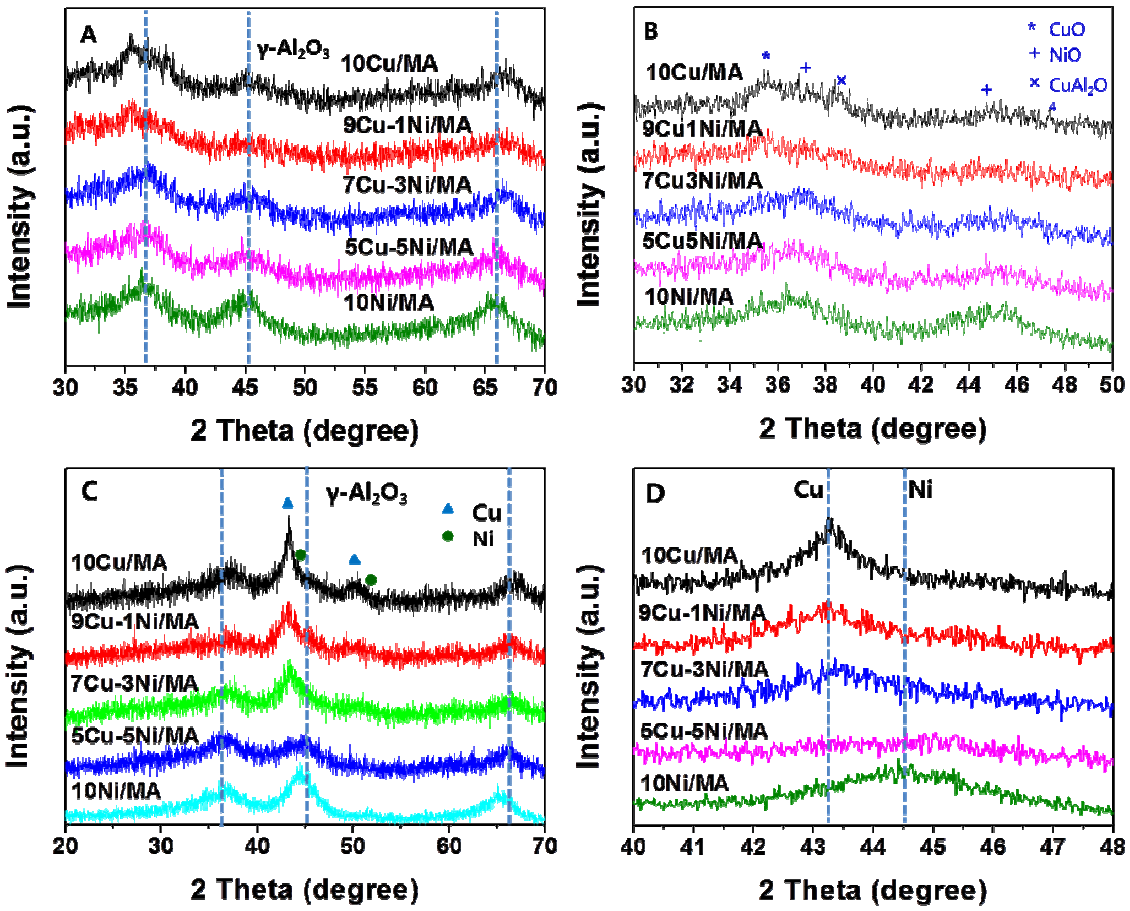

Fig. 4

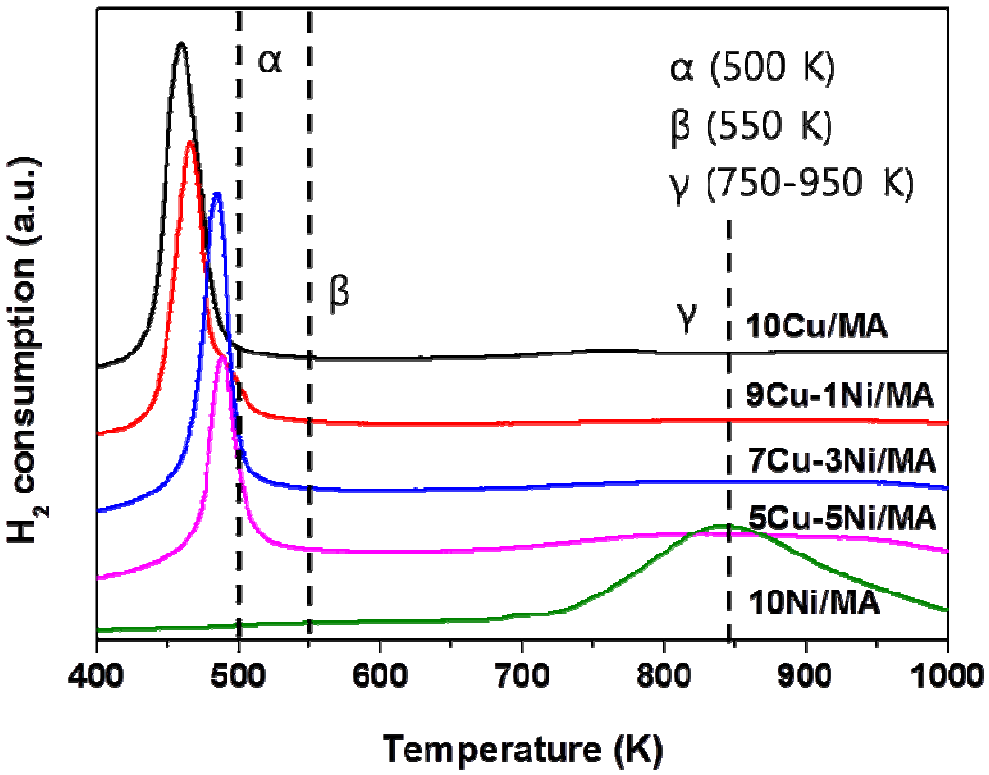

Fig. 5

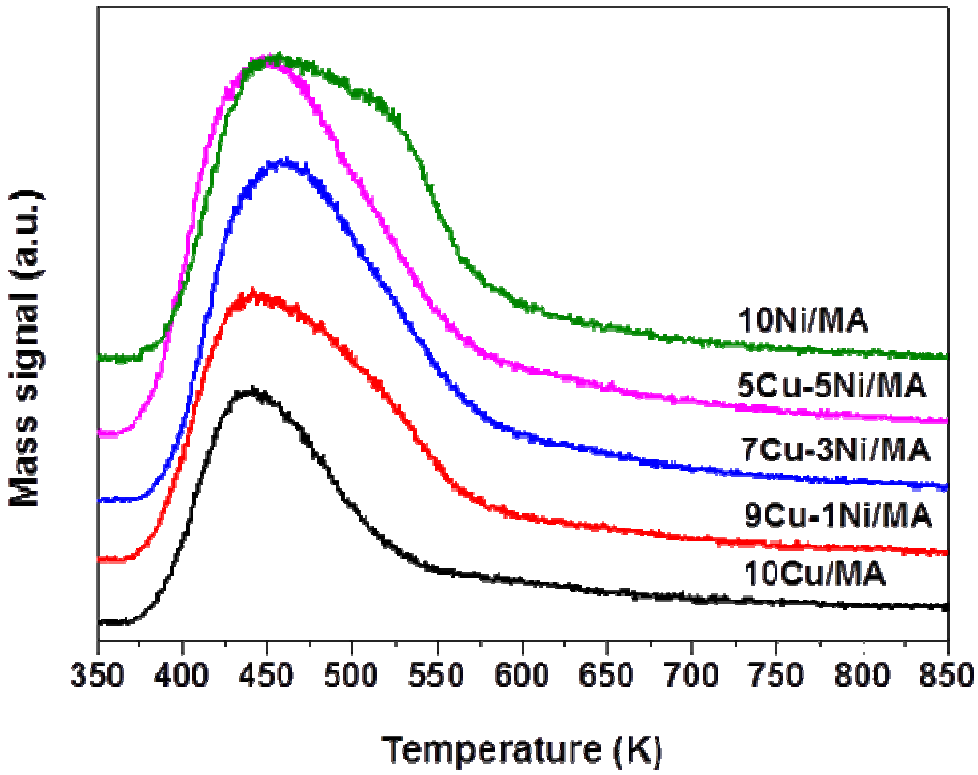

Fig. 6

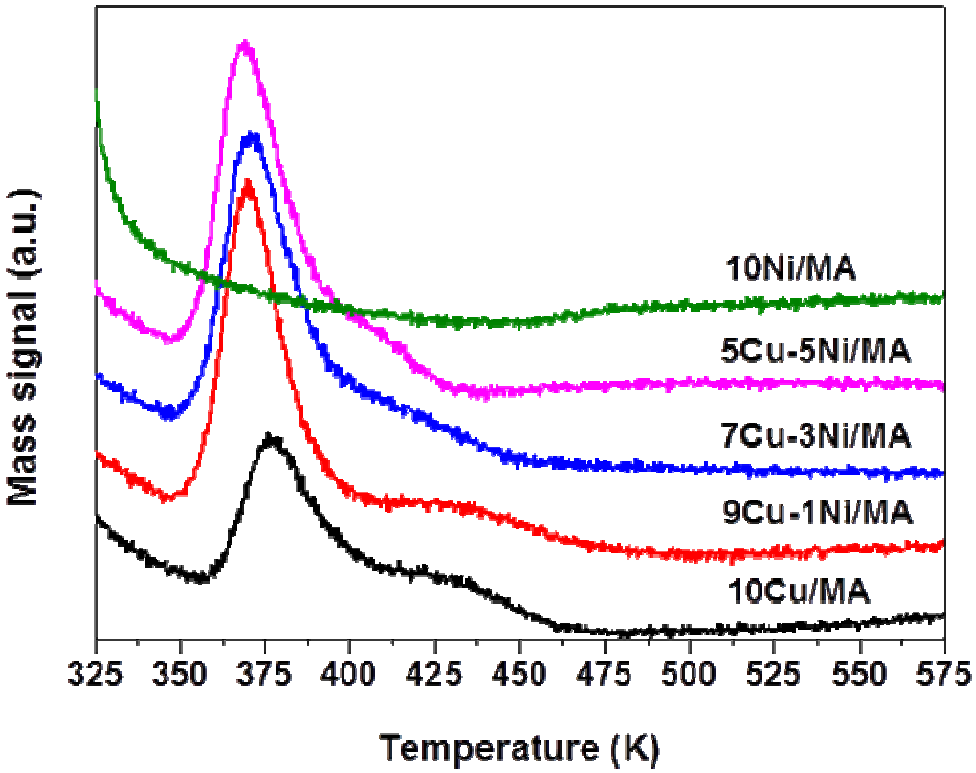

Fig. 7

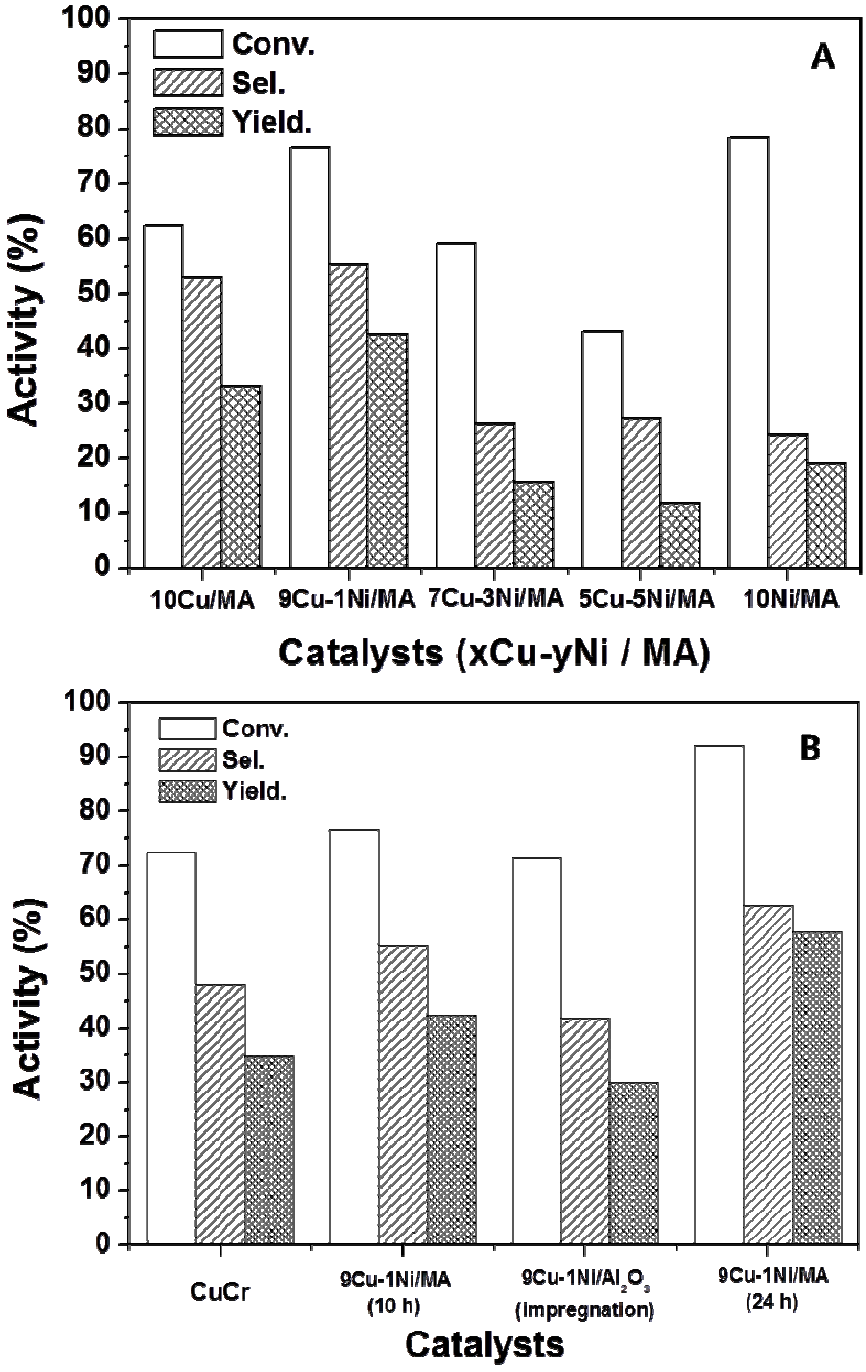

Fig. 8

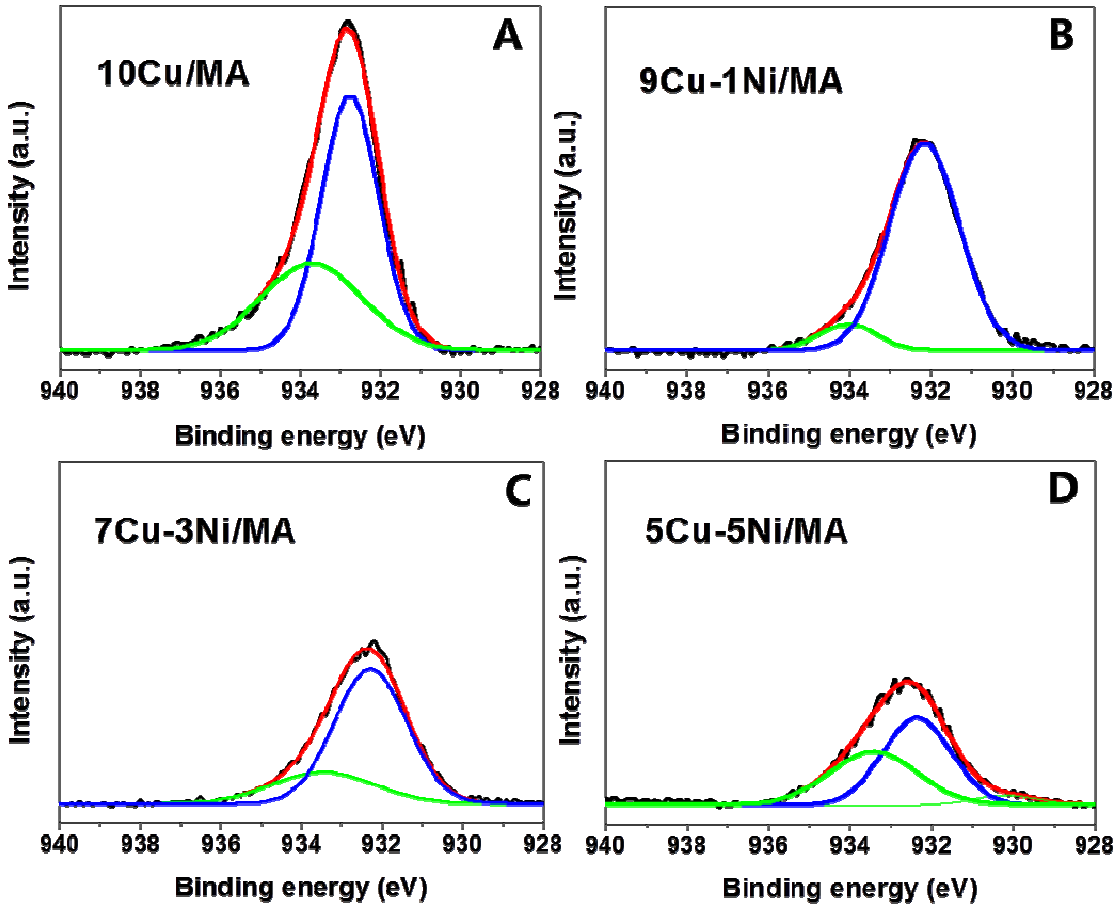

Fig. 9

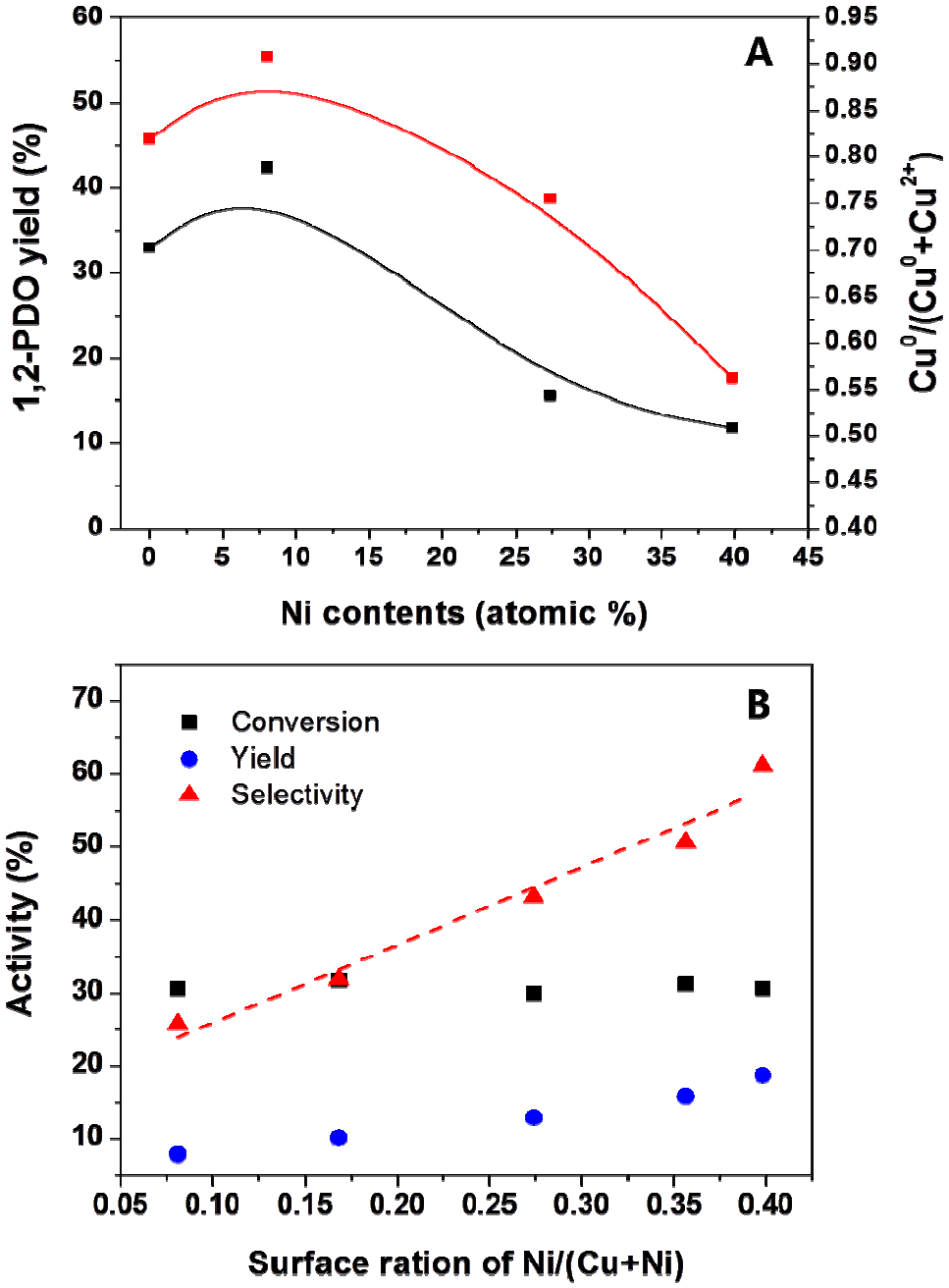

Fig. 10

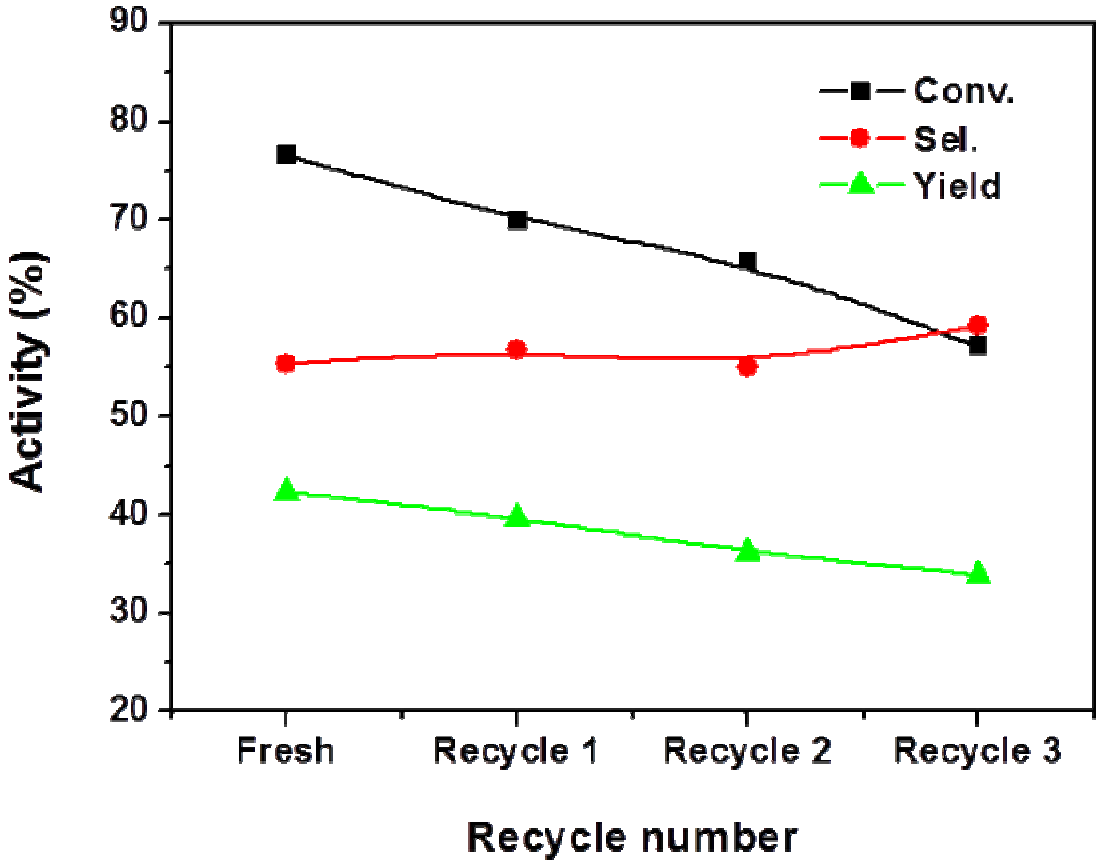

Fig. 11

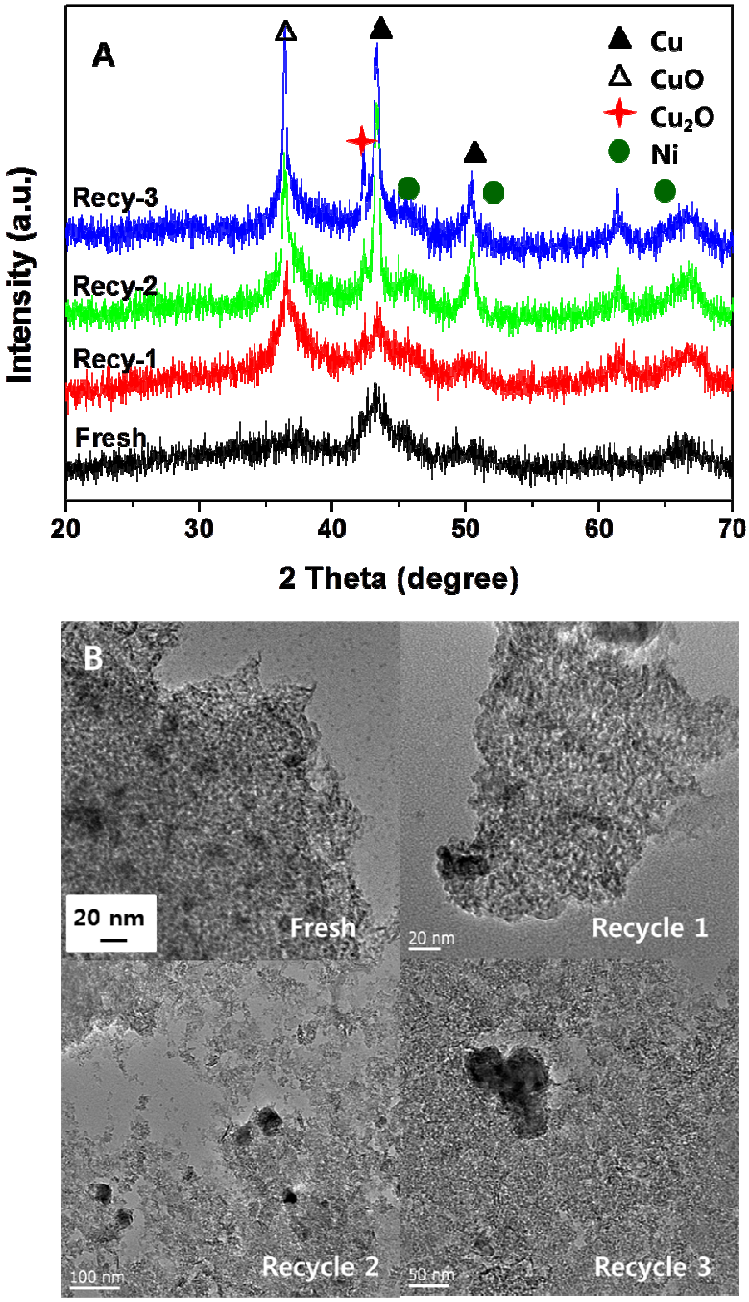

Fig. 12

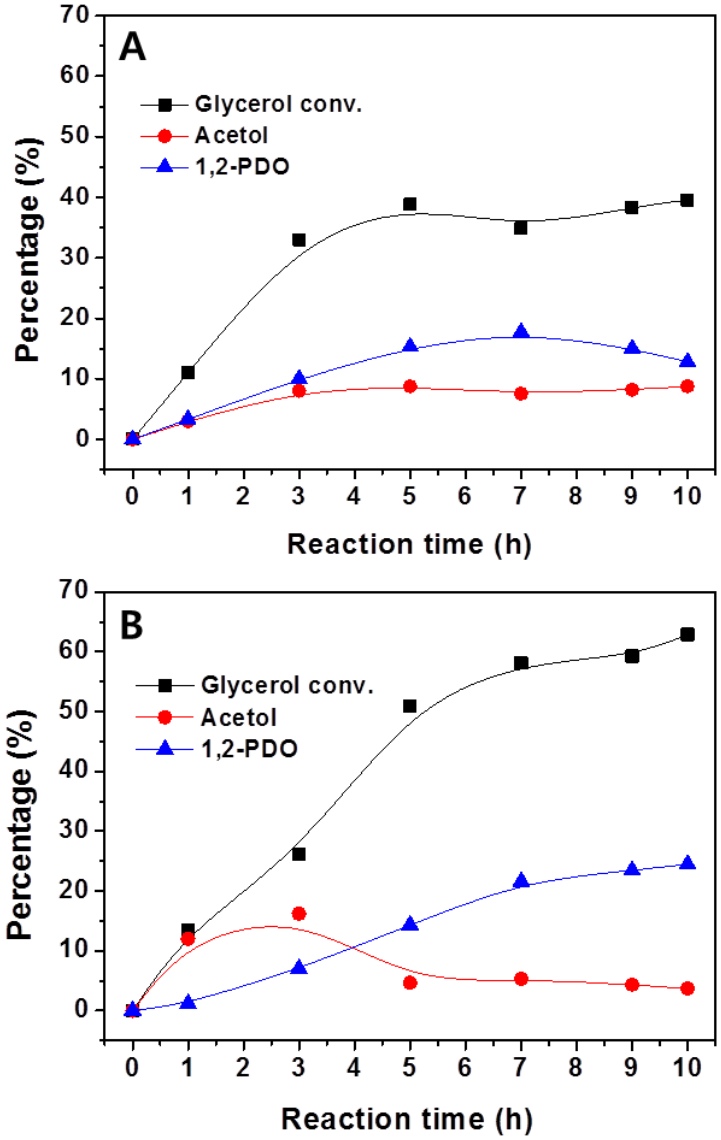

Fig. 13

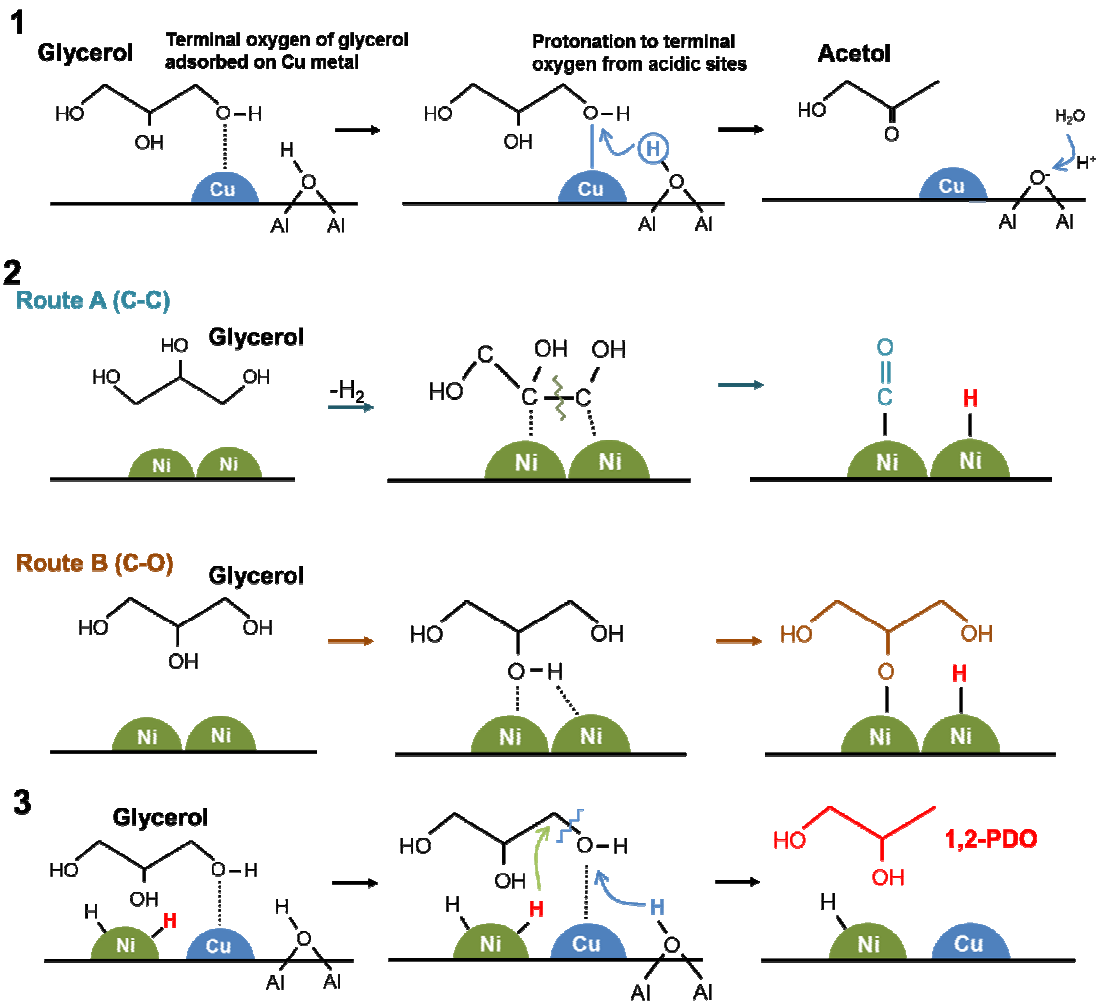

Scheme 1

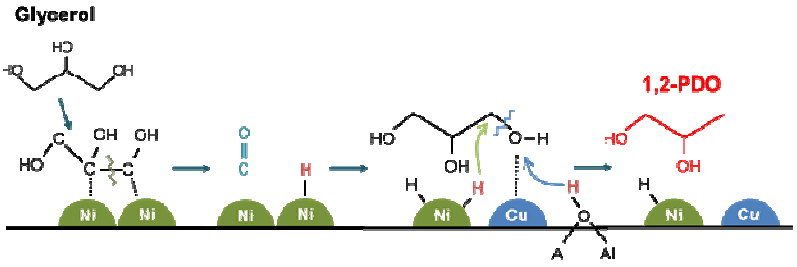

Graphical image